Astrophysical effects on dark matter direct detection

Nassim Bozorgnia

GRAPPA Institute
University of Amsterdam

Based on work done with F. Calore, M. Lovell, G. Bertone, and the EAGLE/APOSTLE teams
1509.02164, 1601.04707

GRAPPA
GRavitation AstroParticle Physics Amsterdam

University of Amsterdam

Dark matter halo

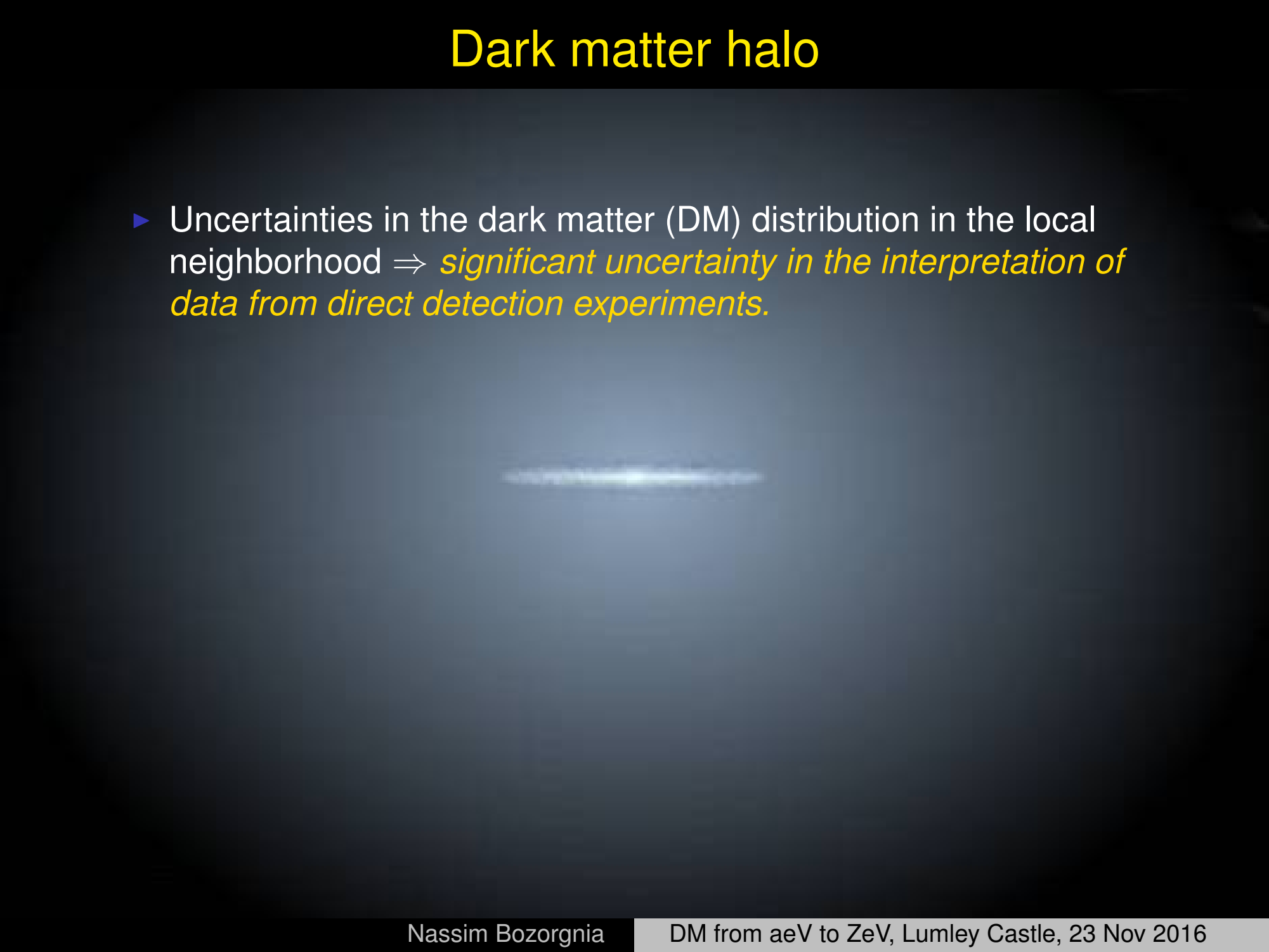

- Uncertainties in the dark matter (DM) distribution in the local neighborhood $\Rightarrow$ *significant uncertainty in the interpretation of data from direct detection experiments.*

Dark matter halo

- Uncertainties in the dark matter (DM) distribution in the local neighborhood $\Rightarrow$ *significant uncertainty in the interpretation of data from direct detection experiments.*

- Usually the **Standard Halo Model (SHM)** is assumed: isothermal sphere with an isotropic Maxwell-Boltzmann velocity distribution.

  - local DM density: $\rho_\chi \sim 0.3$ GeV cm^{-3}
  - typical DM velocity: $\bar{v} \simeq 220$ km/s

Dark matter halo

- Uncertainties in the dark matter (DM) distribution in the local neighborhood $\Rightarrow$ *significant uncertainty in the interpretation of data from direct detection experiments.*

- Usually the **Standard Halo Model (SHM)** is assumed: isothermal sphere with an isotropic Maxwell-Boltzmann velocity distribution.
  - local DM density: $\rho_\chi \sim 0.3$ GeV cm^{-3}
  - typical DM velocity: $\bar{v} \simeq 220$ km/s

- What can we learn from numerical simulations of galaxy formation about the local dark matter distribution?

Dark matter direct detection

- Strong tension between hints for a signal and exclusion limits:

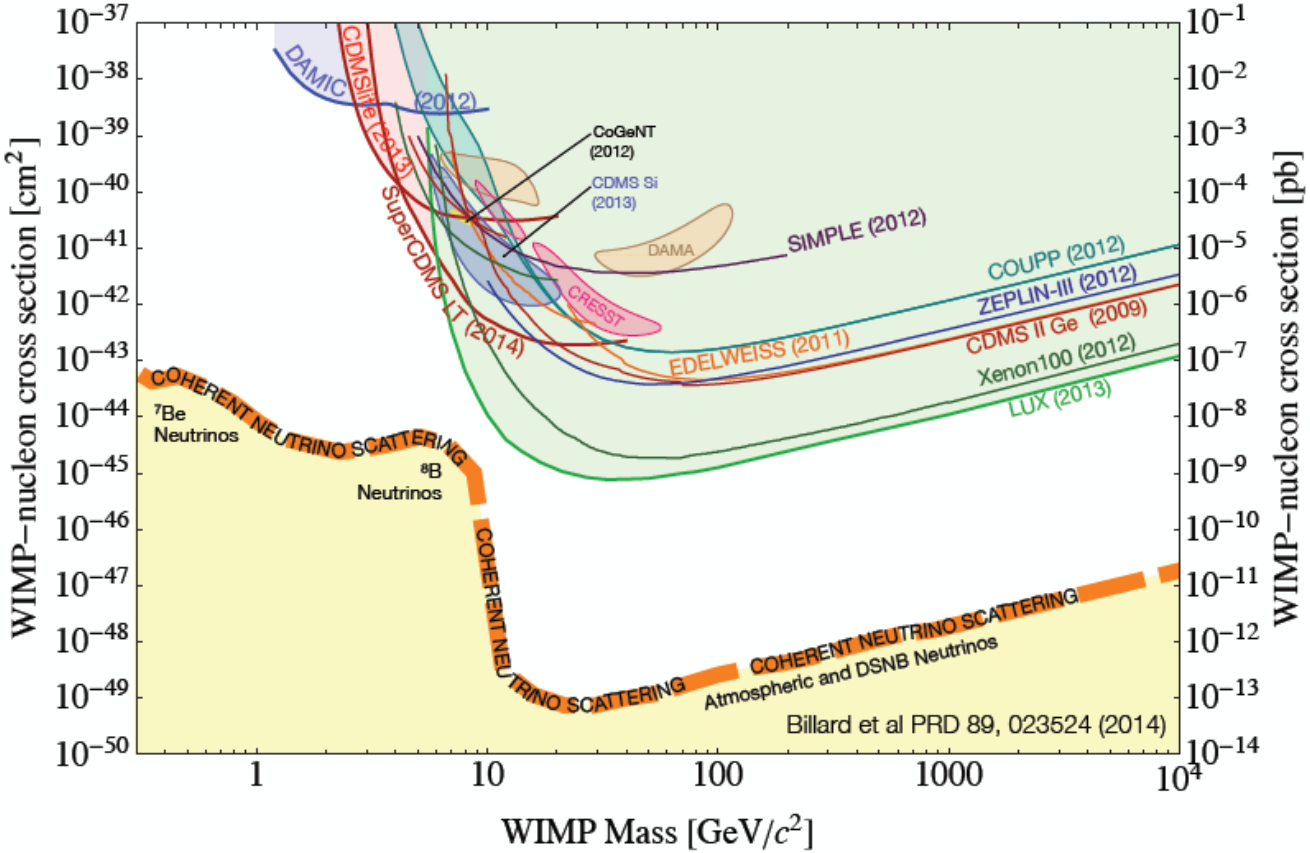

- These kinds of plots assume the Standard Halo Model and a specific DM-nucleus interaction.

The differential event rate

- The differential event rate (event/keV/kg/day):

$$R(E_R, t) = \frac{\rho_\chi}{m_\chi} \frac{1}{m_A} \int_{v>v_m} d^3v \frac{d\sigma_A}{dE_R} \, v \, f_{\rm det}(\mathbf{v}, t)$$

where $v_m = \sqrt{m_A E_R/(2\mu_{\chi A}^2)}$ is the minimum WIMP speed required to produce a recoil energy E_R.

The differential event rate

- The differential event rate (event/keV/kg/day):

$$R(E_R, t) = \frac{\rho_\chi}{m_\chi} \frac{1}{m_A} \int_{v>v_m} d^3v \frac{d\sigma_A}{dE_R} \, v \, f_{\rm det}(\mathbf{v}, t)$$

where $v_m = \sqrt{m_A E_R/(2\mu_{\chi A}^2)}$ is the minimum WIMP speed required to produce a recoil energy E_R.

- For the standard spin-independent and spin-dependent scattering:

$$R(E_R, t) = \underbrace{\frac{\sigma_0 \, F^2(E_R)}{2 m_\chi \mu_{\chi A}^2}}_{\text{particle physics}} \underbrace{\rho_\chi \, \eta(v_m, t)}_{\text{astrophysics}}$$

where

$$\boxed{\eta(v_m, t) \equiv \int_{v>v_m} d^3v \, \frac{f_{\rm det}(\mathbf{v}, t)}{v}} \quad \text{halo integral}$$

Velocity distribution $f_{\rm gal}(\mathbf{v})$?

- The velocity distribution depends on the halo model.

Velocity distribution $f_{\rm gal}(\mathbf{v})$?

- The velocity distribution depends on the halo model.
- In the SHM, a truncated Maxwellian velocity distribution is assumed:

$$f_{\rm gal}(\mathbf{v}) \approx \begin{cases} N \exp(-\mathbf{v}^2/\bar{v}^2) & v < v_{\rm esc} \\ 0 & v \geq v_{\rm esc} \end{cases}$$

with $\bar{v} \simeq 220$ km/s, $v_{\rm esc} = 550$ km/s.

Velocity distribution $f_{\rm gal}(\mathbf{v})$?

- The velocity distribution depends on the halo model.
- In the SHM, a truncated Maxwellian velocity distribution is assumed:

$$f_{\rm gal}(\mathbf{v}) \approx \begin{cases} N \exp(-\mathbf{v}^2/\bar{v}^2) & v < v_{\rm esc} \\ 0 & v \geq v_{\rm esc} \end{cases}$$

  with $\bar{v} \simeq 220$ km/s, $v_{\rm esc} = 550$ km/s.

- DM distribution could be very different from Maxwellian:
  - Most likely both smooth and un-virialized (streams and debris flows) components.
  - the smooth component may not be Maxwellian.

Velocity distribution from simulations

- DM velocity distributions from cosmological N-body simulations **without baryons**, deviate substantially from a Maxwellian.

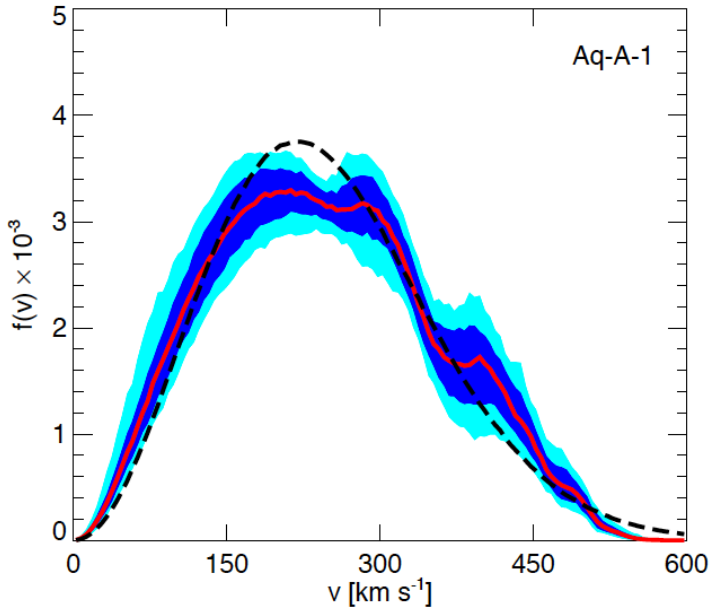

Vogelsberger et al. 0812.0362

Velocity distribution from simulations

- DM velocity distributions from cosmological N-body simulations **without baryons**, deviate substantially from a Maxwellian.

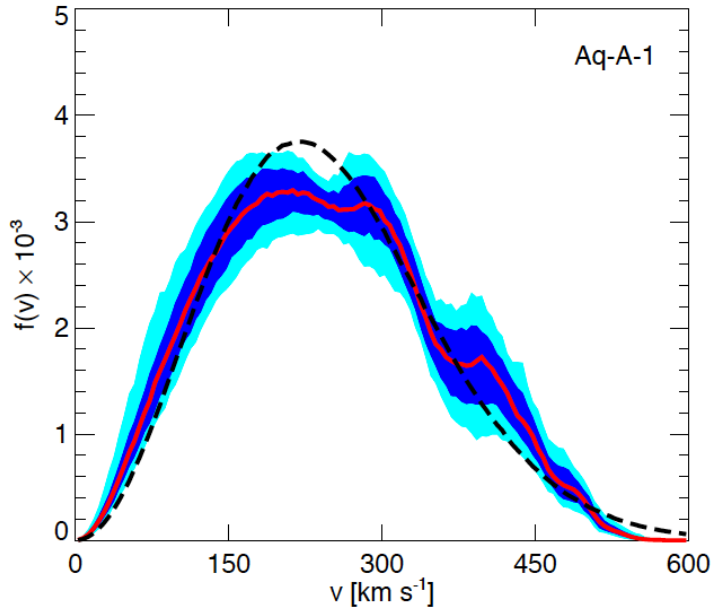

Vogelsberger et al. 0812.0362

- Significant systematic uncertainties since the impact of baryons are neglected.
- Realistic cosmological simulations **with baryons** have recently become possible!

Our aim

- Identify Milky Way-like galaxies in high resolution hydrodynamic simulations, by taking into account observational constraints on the Milky Way (MW).
- Extract the local DM density and velocity distribution for the selected MW analogues.
- Analyze the data from direct detection experiments, using the predicted local DM distributions of the selected haloes.

Hydrodynamic simulations

- We use the **EAGLE** and **APOSTLE** hydrodynamic simulations (**DM** $+$ **baryons**).

Name	L (Mpc)	N	$m_{\rm g}$ $(\mathrm{M}_\odot)$	$m_{\rm dm}$ $(\mathrm{M}_\odot)$
EAGLE IR	100	6.8×10^9	1.81×10^6	9.70×10^6
EAGLE HR	25	8.5×10^8	2.26×10^5	1.21×10^6
APOSTLE IR	–	–	1.3×10^5	5.9×10^5

- **APOSTLE IR**: zoomed simulations of Local Group-analogue systems, comparable in resolution to **EAGLE HR**.

Hydrodynamic simulations

- We use the **EAGLE** and **APOSTLE** hydrodynamic simulations (**DM** + **baryons**).

Name	L (Mpc)	N	$m_{\rm g}$ ($\rm M_\odot$)	$m_{\rm dm}$ ($\rm M_\odot$)
EAGLE IR	100	6.8×10^9	1.81×10^6	9.70×10^6
EAGLE HR	25	8.5×10^8	2.26×10^5	1.21×10^6
APOSTLE IR	–	–	1.3×10^5	5.9×10^5

- **APOSTLE IR**: zoomed simulations of Local Group-analogue systems, comparable in resolution to **EAGLE HR**.
- These simulations are calibrated to reproduce the observed distribution of stellar masses and sizes of low-redshift galaxies.

Hydrodynamic simulations

- We use the **EAGLE** and **APOSTLE** hydrodynamic simulations (**DM** + **baryons**).

Name	L (Mpc)	N	$m_{\rm g}$ ($\rm M_\odot$)	$m_{\rm dm}$ ($\rm M_\odot$)
EAGLE IR	100	6.8×10^9	1.81×10^6	9.70×10^6
EAGLE HR	25	8.5×10^8	2.26×10^5	1.21×10^6
APOSTLE IR	–	–	1.3×10^5	5.9×10^5

- **APOSTLE IR**: zoomed simulations of Local Group-analogue systems, comparable in resolution to **EAGLE HR**.
- These simulations are calibrated to reproduce the observed distribution of stellar masses and sizes of low-redshift galaxies.
- Companion dark matter only (DMO) simulations were run assuming all the matter content is collisionless.

EAGLE simulations

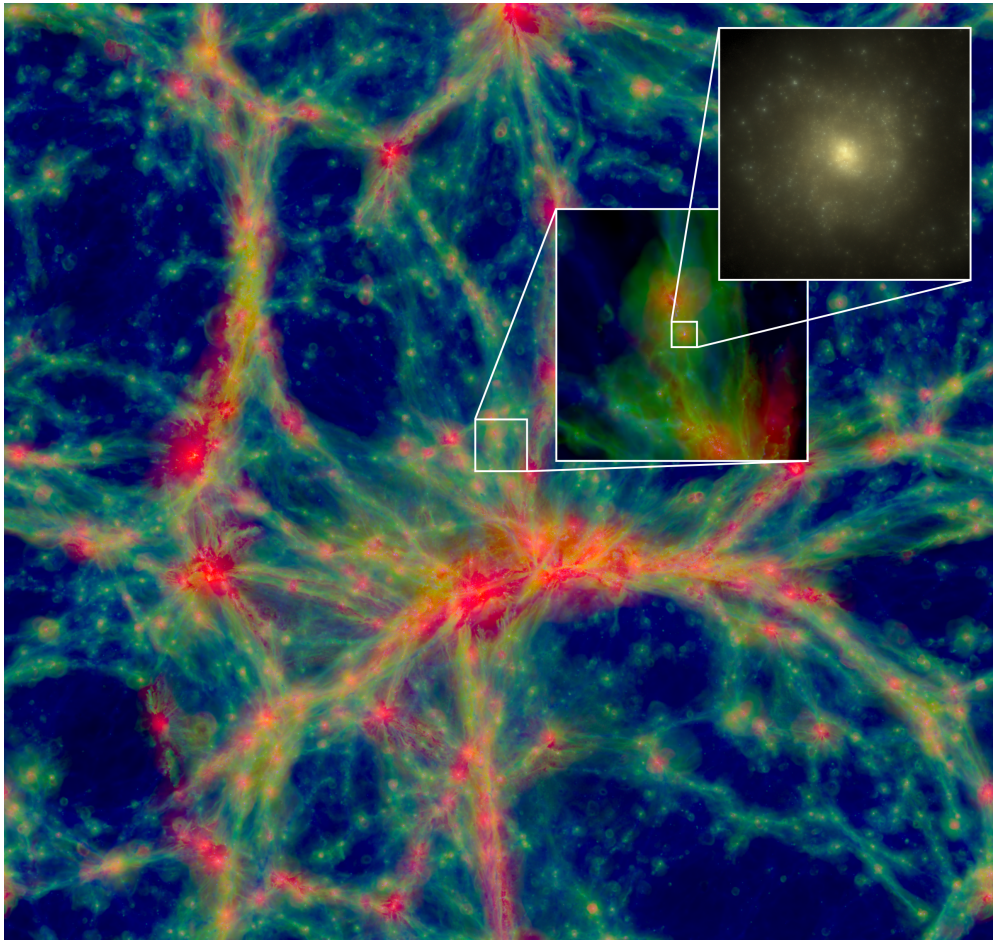

EAGLE project, 1407.7040

Intergalactic gas: blue $\Rightarrow$ green $\Rightarrow$ red with increasing temperature.

Milky Way analogues

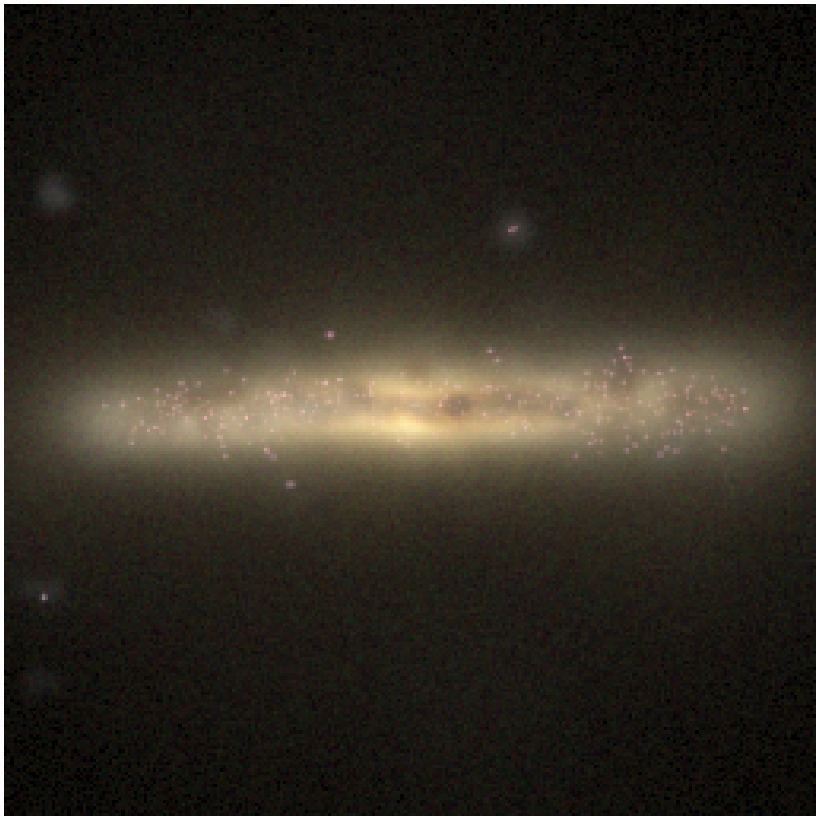

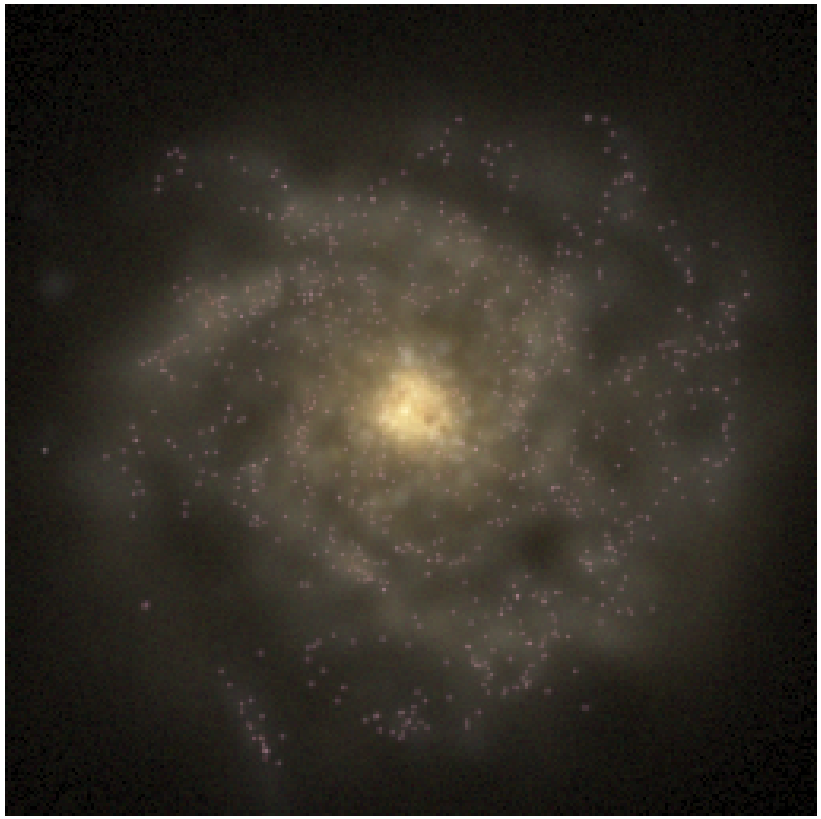

Identifying Milky Way analogues

- Usually a simulated halo is classified as *MW-like* if it satisfies the MW mass constraint, which has a large uncertainty. We show that the mass constraint is not enough to define a MW-like galaxy.

Identifying Milky Way analogues

- Usually a simulated halo is classified as *MW-like* if it satisfies the MW mass constraint, which has a large uncertainty. We show that the mass constraint is not enough to define a MW-like galaxy.

- Consider simulated haloes with $5 \times 10^{11} < M_{200}/\mathrm{M}_{\odot} < 2 \times 10^{13}$ and select the galaxies which most closely resemble the MW by the following criteria:

  - Rotation curve from simulation fits well the observed MW kinematical data from: **Iocco, Pato, Bertone, 1502.03821**.
  - The total stellar mass of the simulated galaxies is within the 3σ observed MW range: $4.5 \times 10^{10} < M_{*}/\mathrm{M}_{\odot} < 8.3 \times 10^{10}$.

Observations vs. simulations

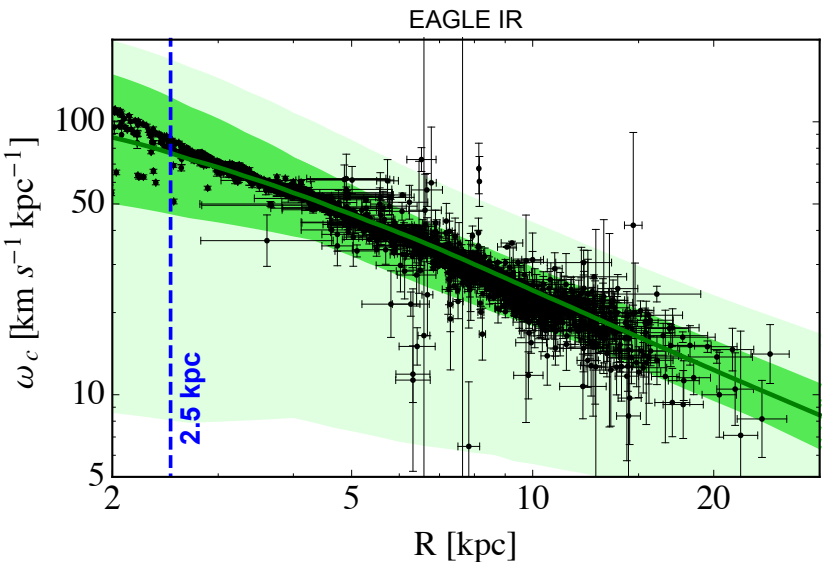

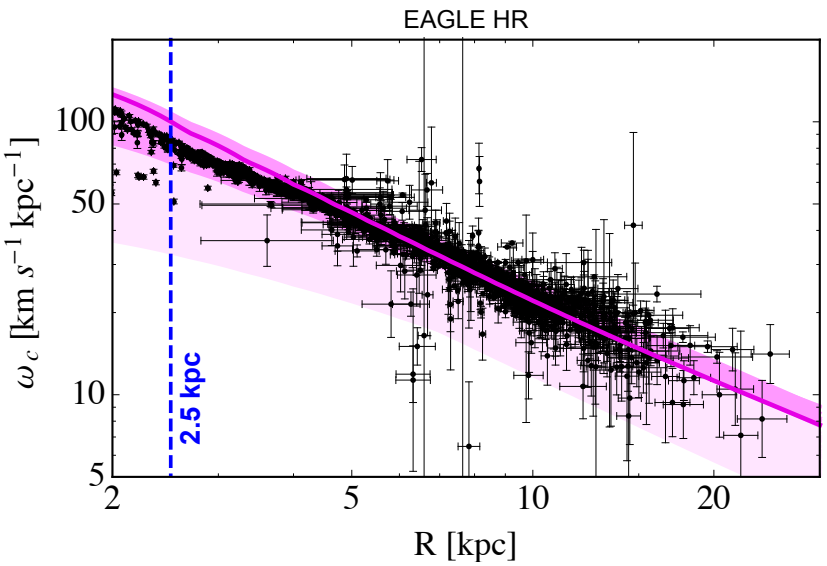

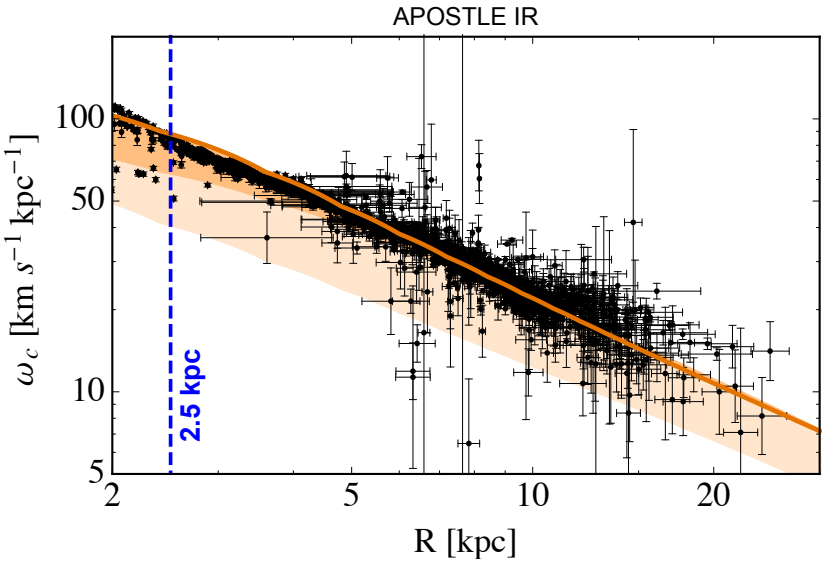

Initial sets of haloes:

EAGLE IR: 2411 | **EAGLE HR: 61** |

APOSTLE IR: 24

Haloes which have correct total stellar mass:

EAGLE IR: 335 | **EAGLE HR: 12** |

APOSTLE IR: 2

Observations vs. simulations

Goodness of fit to the observed data:

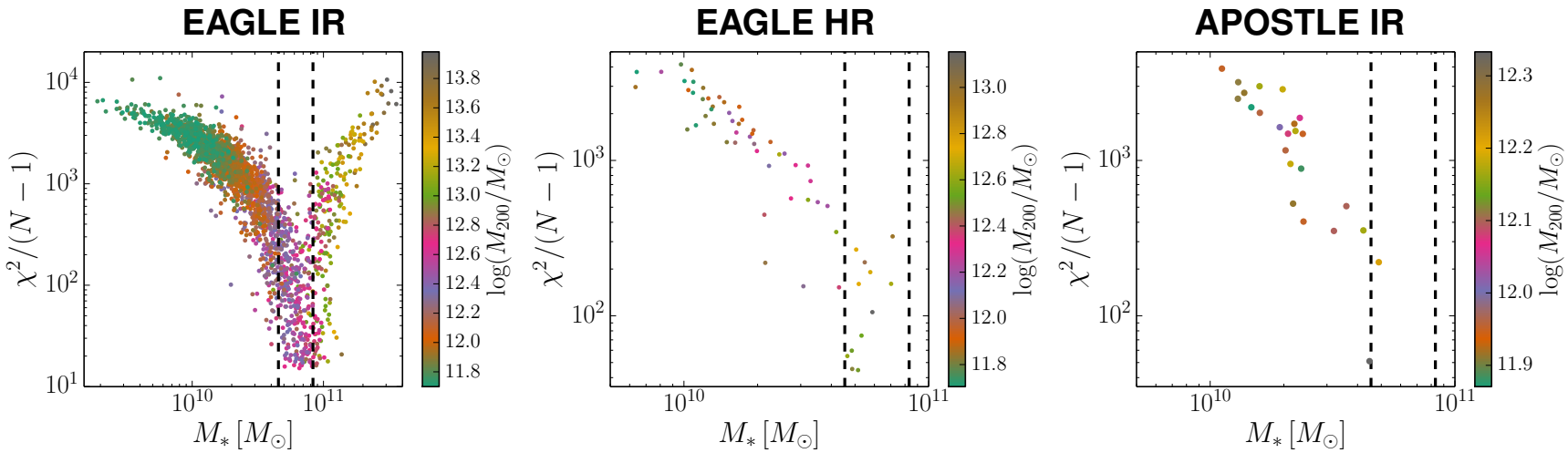

$N = 2687$ is the total number of observational data points used.

- Minimum of the reduced χ^2 occurs within the 3σ measured range of the MW total stellar mass. $\Rightarrow$ haloes with correct MW stellar mass have rotation curves which match well the observations.

Observations vs. simulations

Goodness of fit to the observed data:

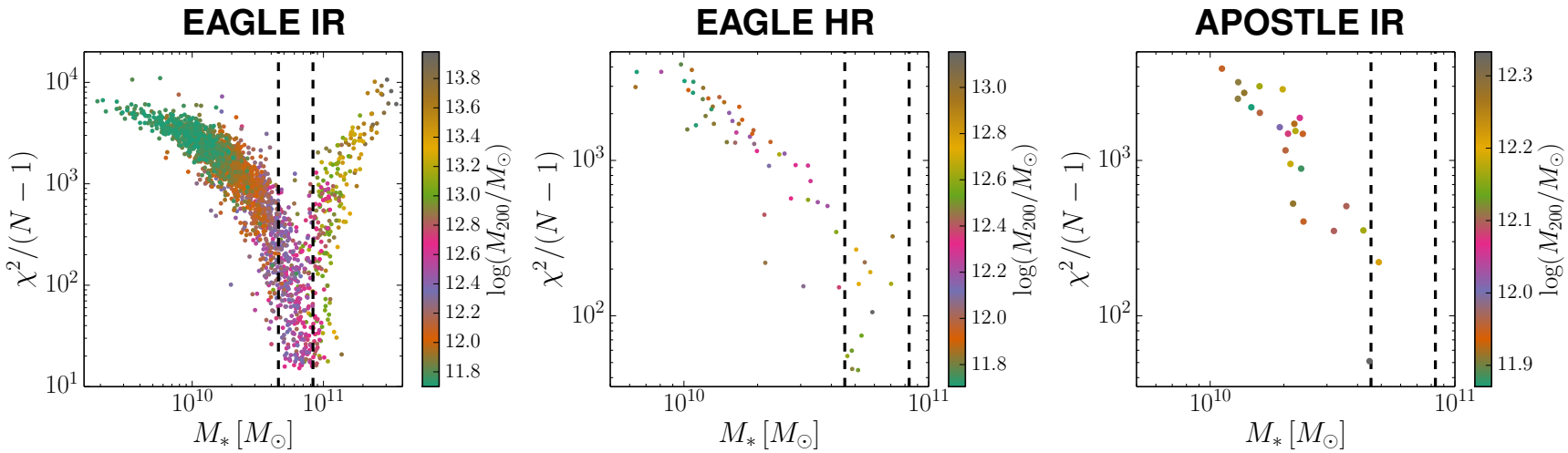

$N = 2687$ is the total number of observational data points used.

- Minimum of the reduced χ^2 occurs within the 3σ measured range of the MW total stellar mass. $\Rightarrow$ haloes with correct MW stellar mass have rotation curves which match well the observations.
- We focus only on the selected **EAGLE HR** and **APOSTLE IR** haloes due to higher resolution $\Rightarrow$ total of **14** MW analogues.

Dark matter density profiles

- Spherically averaged DM density profiles:

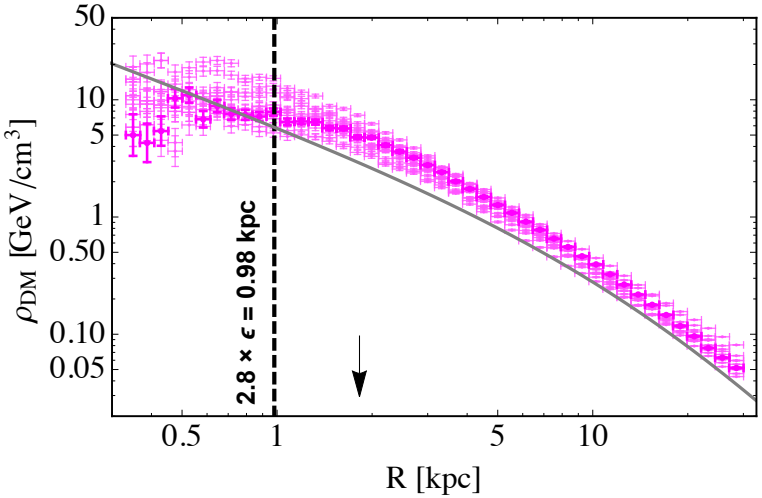

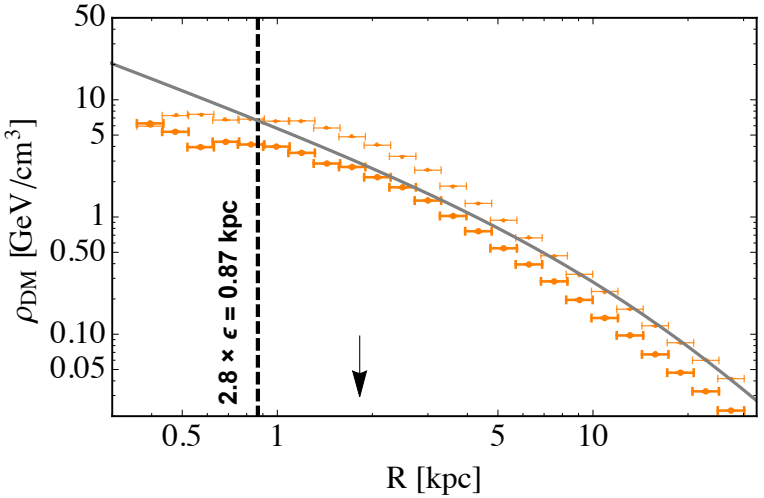

Dark matter density profiles

- Spherically averaged DM density profiles:

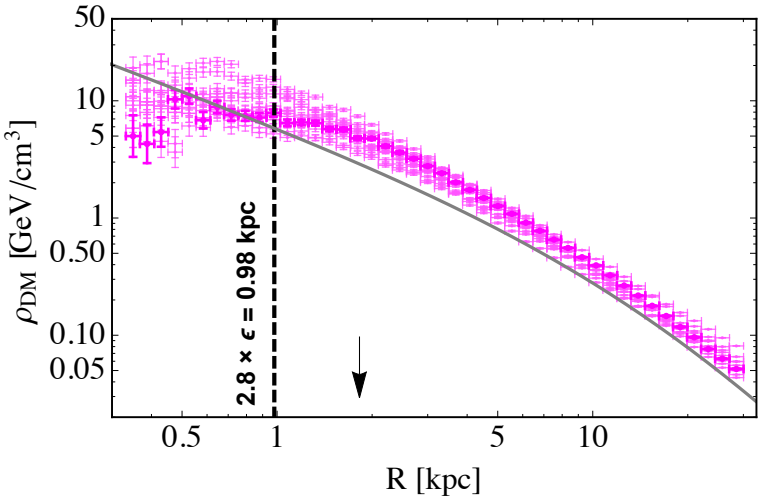

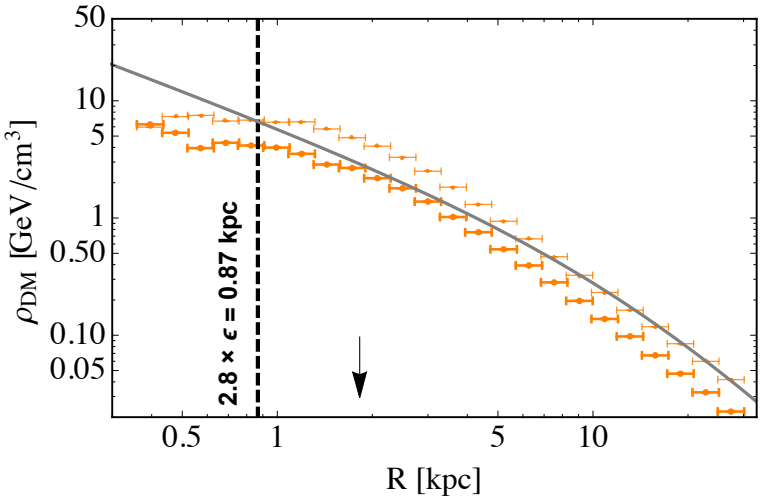

- Need the DM density at the position of the Sun.
- Consider a torus aligned with the stellar disc with $7\ \mathrm{kpc} < R < 9\ \mathrm{kpc}$, and $-1\ \mathrm{kpc} < z < 1\ \mathrm{kpc}$.

EAGLE HR: local $\rho_{\mathrm{DM}} = 0.42 - 0.73\ \mathrm{GeV\ cm^{-3}}$.

APOSTLE IR: local $\rho_{\mathrm{DM}} = 0.41 - 0.54\ \mathrm{GeV\ cm^{-3}}$.

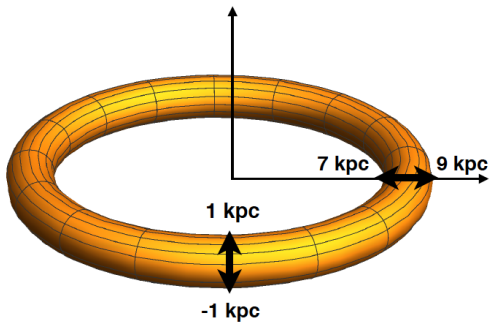

Local speed distributions

In the galactic rest frame:

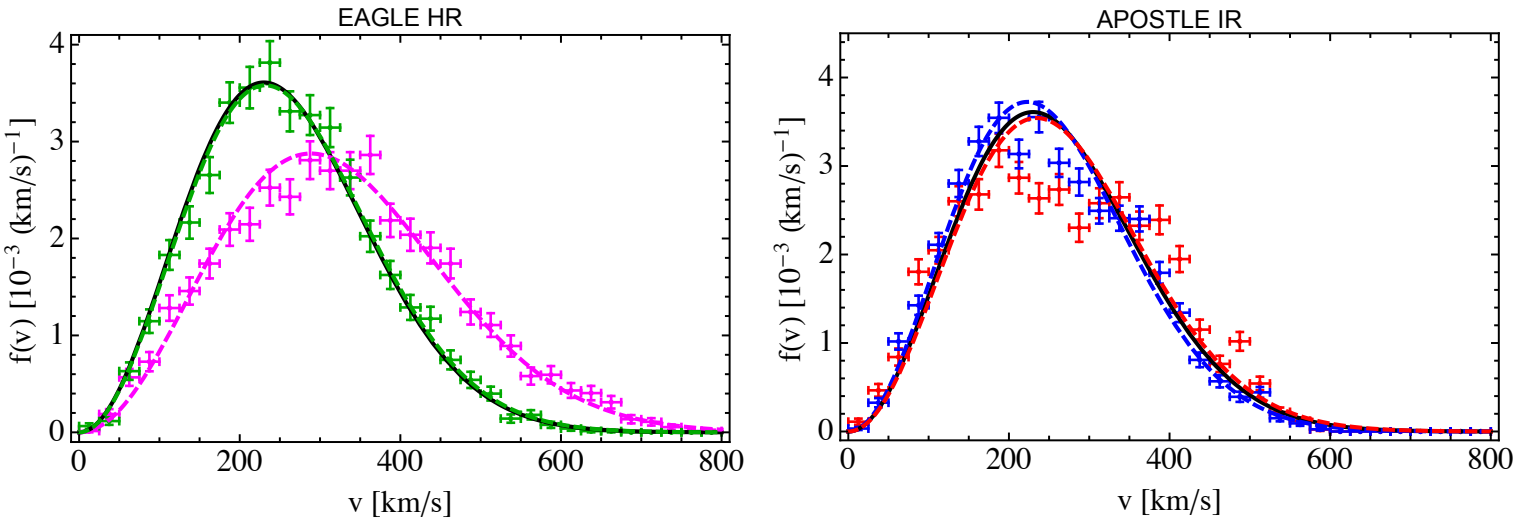

Local speed distributions

In the galactic rest frame:

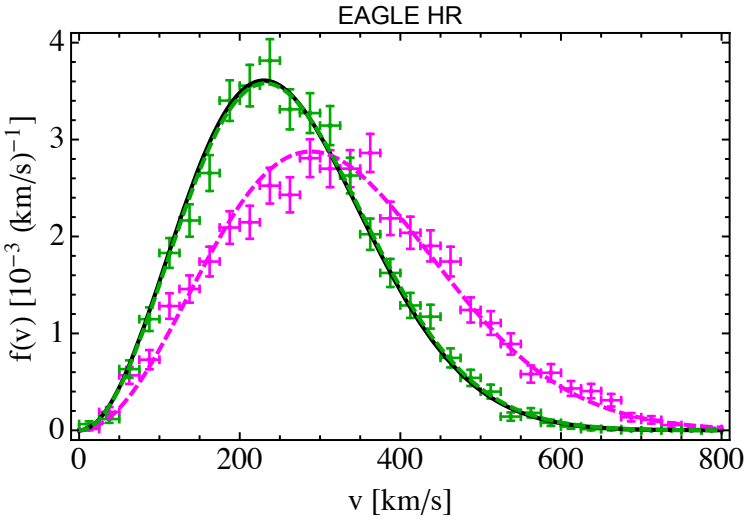

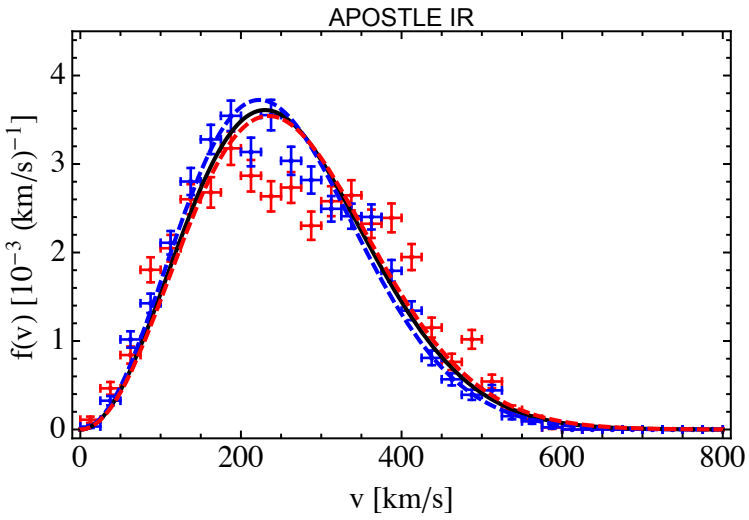

- Comparison to DMO simulations:

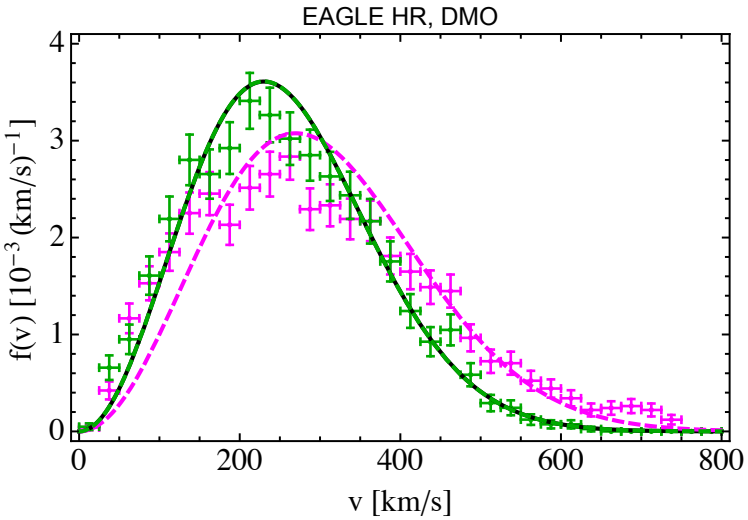

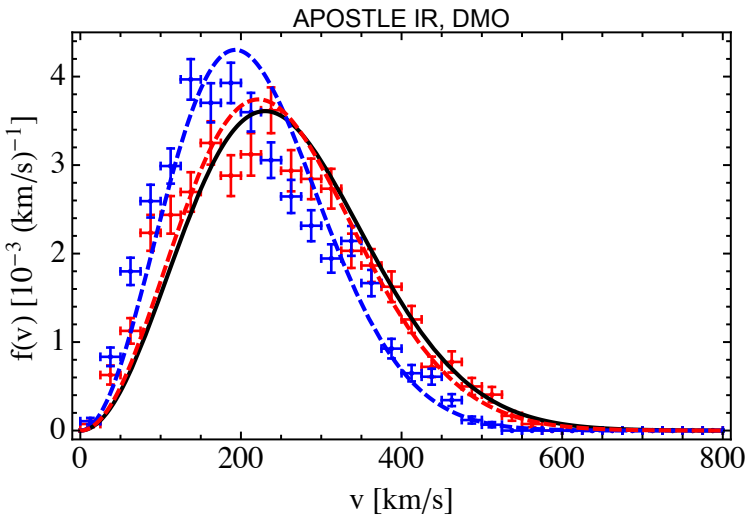

Local DM speed distribution

- Baryons deepen the gravitational potential of the Galaxy in the inner regions, resulting in more high velocity particles. $\Rightarrow$ The peak of the DM speed distribution is shifted to higher speeds when baryons are included in the simulations.

Local DM speed distribution

- Baryons deepen the gravitational potential of the Galaxy in the inner regions, resulting in more high velocity particles. $\Rightarrow$ The peak of the DM speed distribution is shifted to higher speeds when baryons are included in the simulations.
- The Maxwellian distribution with a free peak provides a better fit to most haloes in the hydrodynamic simulations compared to their DMO counterparts.

Local DM speed distribution

- Baryons deepen the gravitational potential of the Galaxy in the inner regions, resulting in more high velocity particles. $\Rightarrow$ The peak of the DM speed distribution is shifted to higher speeds when baryons are included in the simulations.
- The Maxwellian distribution with a free peak provides a better fit to most haloes in the hydrodynamic simulations compared to their DMO counterparts.
- The best fit peak speed of the Maxwellian distribution in the hydrodynamic simulations: 223 – 289 km/s.

Components of the velocity distribution

Distributions of radial, azimuthal, and vertical velocity components:

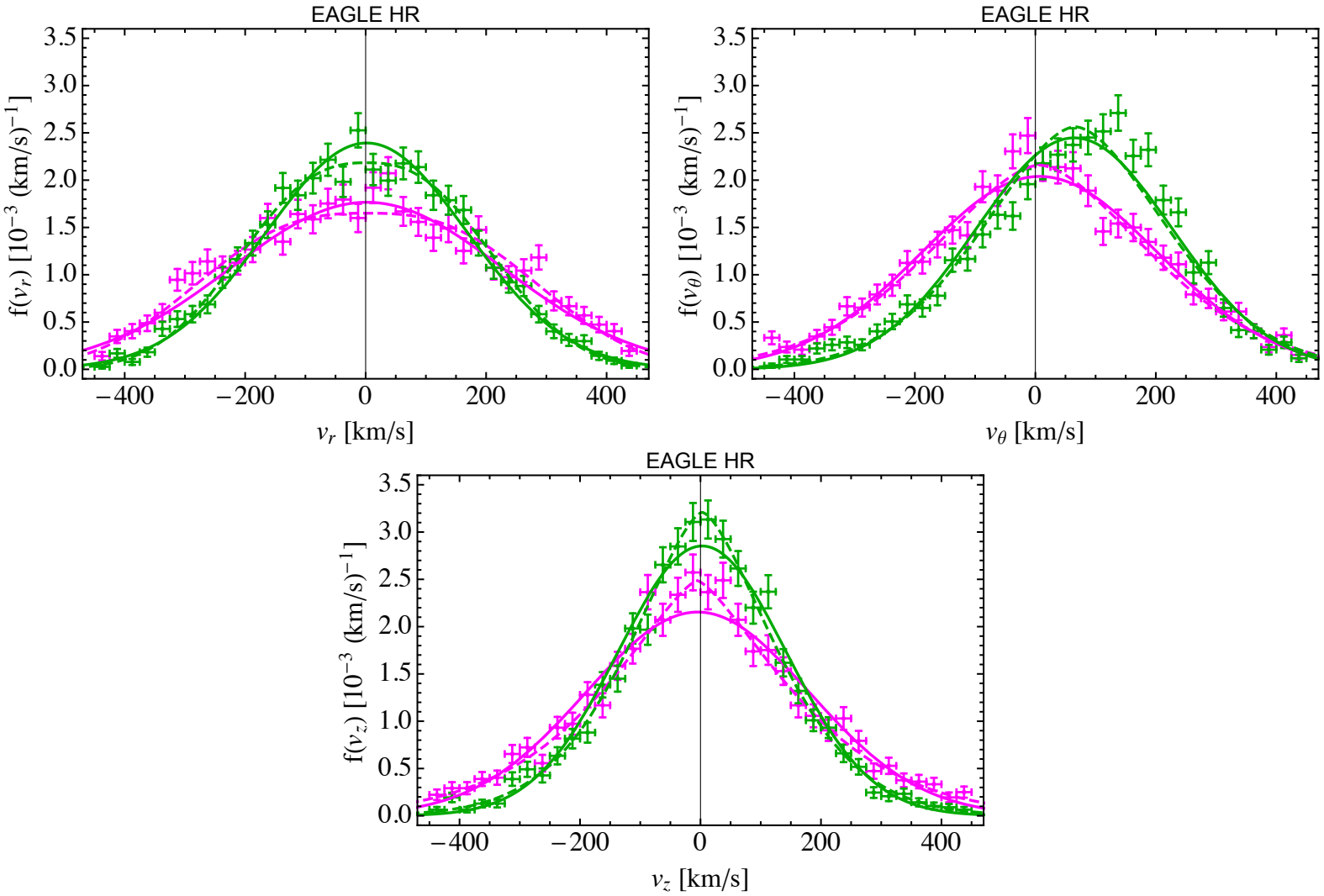

Components of the velocity distribution

Comparison to DMO simulations:

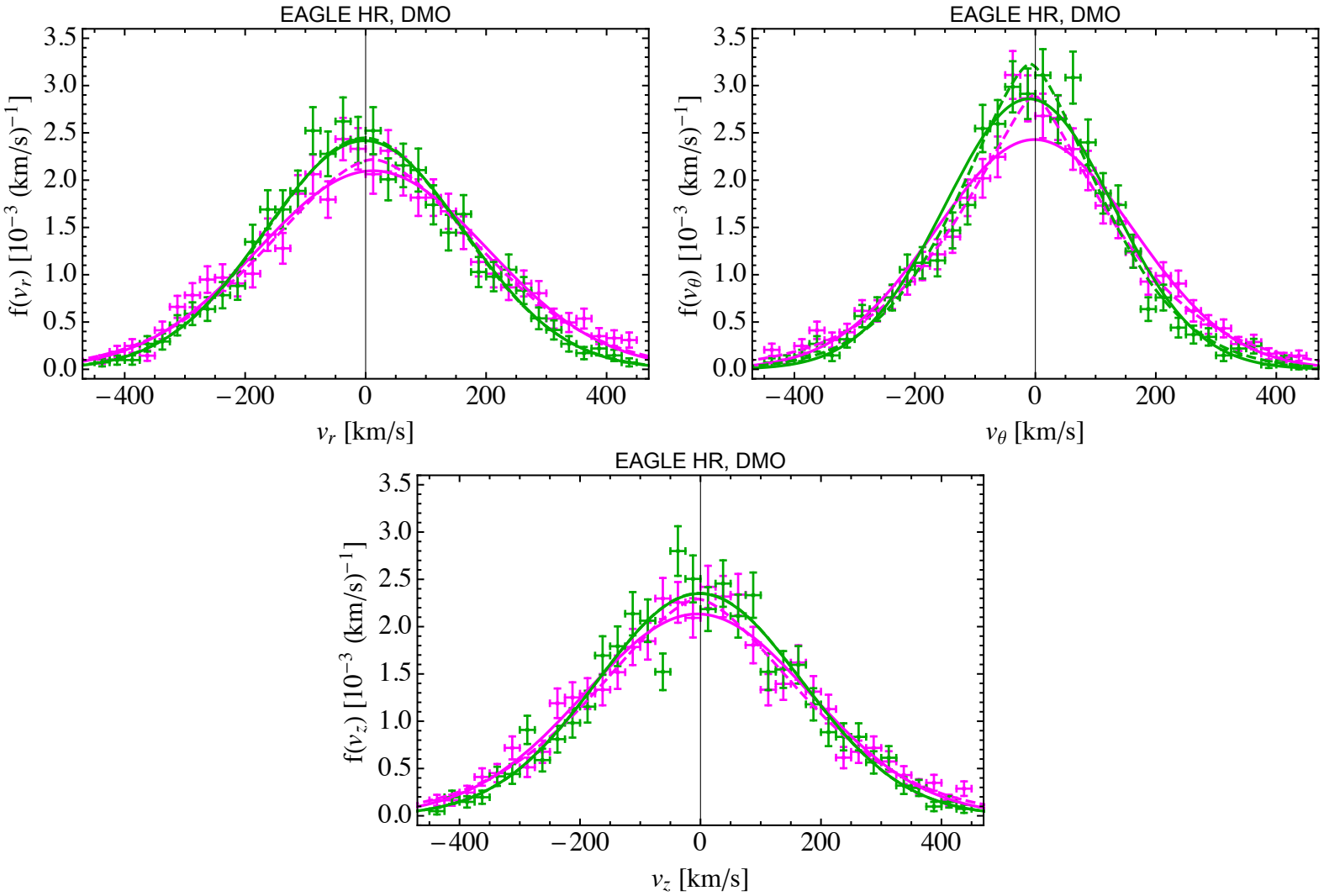

Components of the velocity distribution

- The three components of the DM velocity distribution are not similar. $\Rightarrow$ clear velocity anisotropy at the Solar circle.
- The distributions of the **radial** and **vertical** velocity components are peaked around zero.

Components of the velocity distribution

- The three components of the DM velocity distribution are not similar. $\Rightarrow$ clear velocity anisotropy at the Solar circle.
- The distributions of the **radial** and **vertical** velocity components are peaked around zero.
- Four haloes have a significant positive mean **azimuthal** speed ($\mu > 20$ km/s). The DMO counterparts of these haloes don't show evidence of rotation.

Components of the velocity distribution

- The three components of the DM velocity distribution are not similar. $\Rightarrow$ clear velocity anisotropy at the Solar circle.
- The distributions of the **radial** and **vertical** velocity components are peaked around zero.
- Four haloes have a significant positive mean **azimuthal** speed ($\mu > 20$ km/s). The DMO counterparts of these haloes don't show evidence of rotation.
- Is this pointing to the existence of a "dark disc"?
  - Among the four rotating haloes, two haloes have a rotating DM component in the disc with mean velocity comparable (within 50 km/s) to that of the stars.
  - Hint for the existence of a co-rotating dark disc in two out of 14 MW-like haloes. $\Rightarrow$ dark discs are relatively rare in our halo sample.

The halo integral

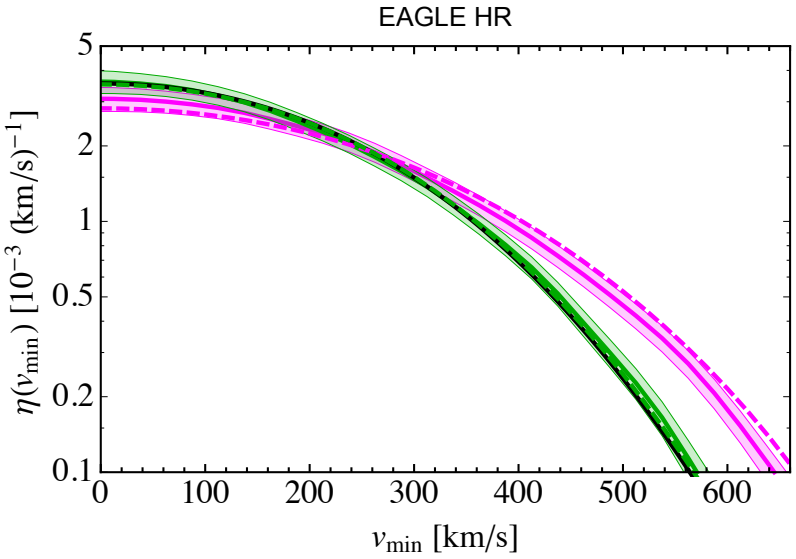

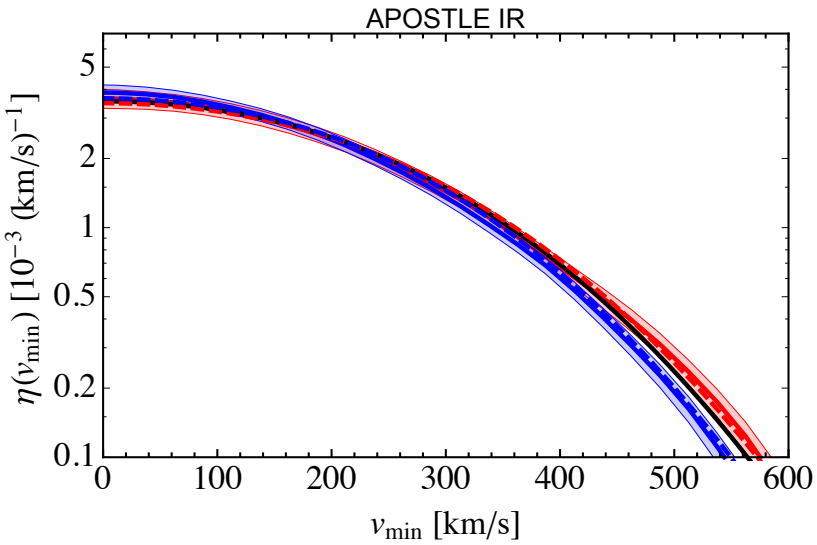

The halo integral

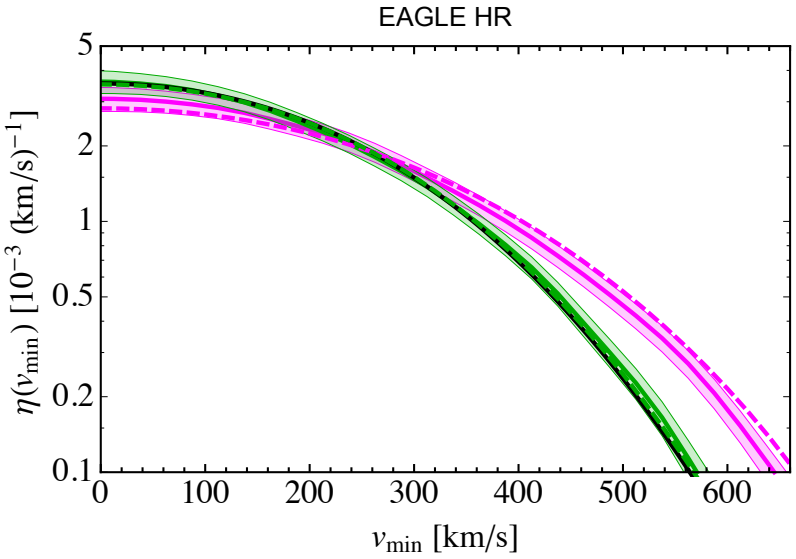

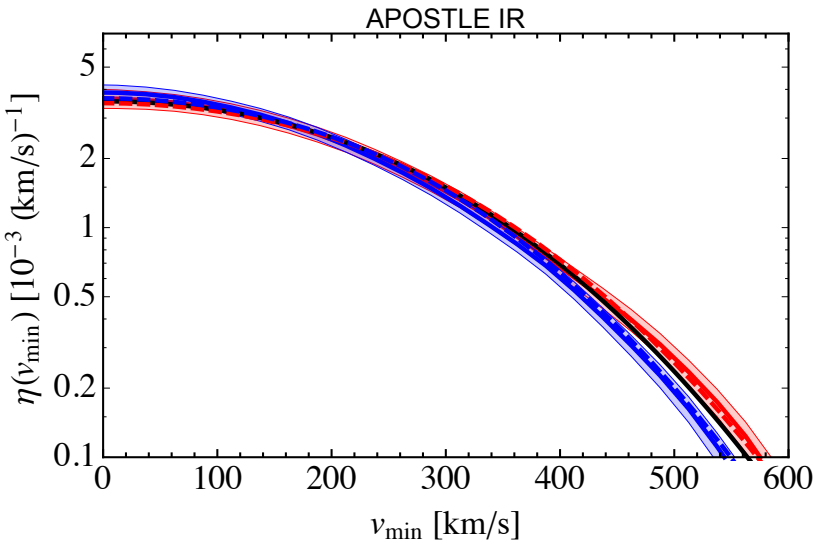

- Significant halo-to-halo scatter in the halo integrals.

The halo integral

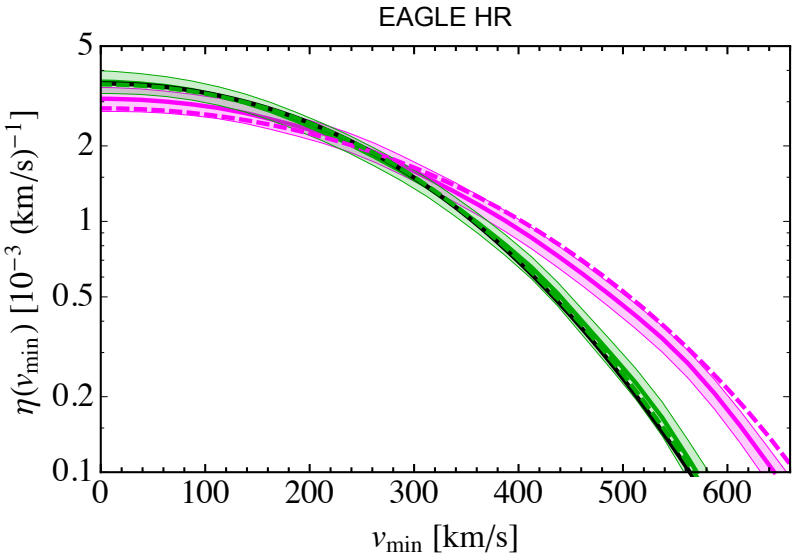

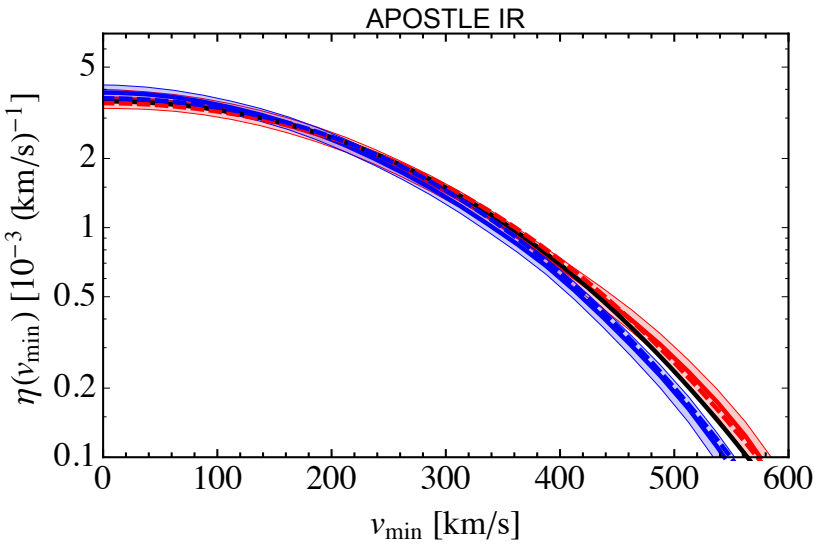

- Significant halo-to-halo scatter in the halo integrals.
- Halo integrals for the best fit Maxwellian velocity distribution fall within the 1σ uncertainty band of the halo integrals of the simulated haloes.

The halo integral

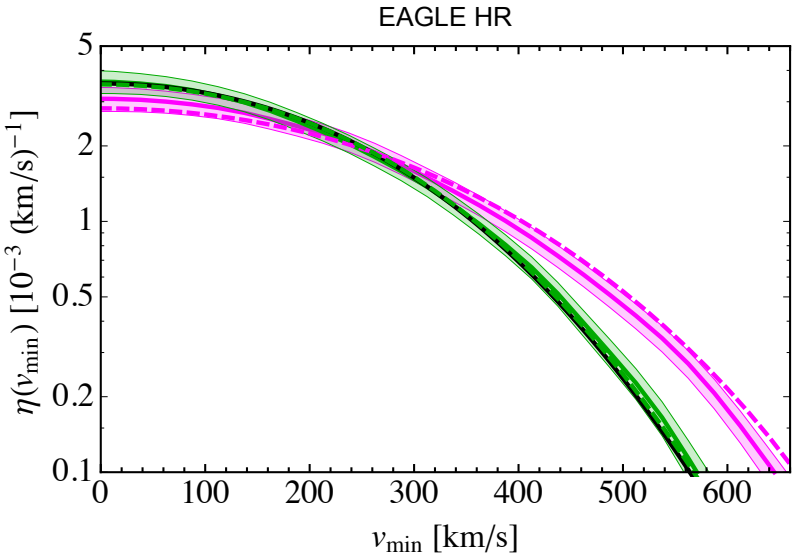

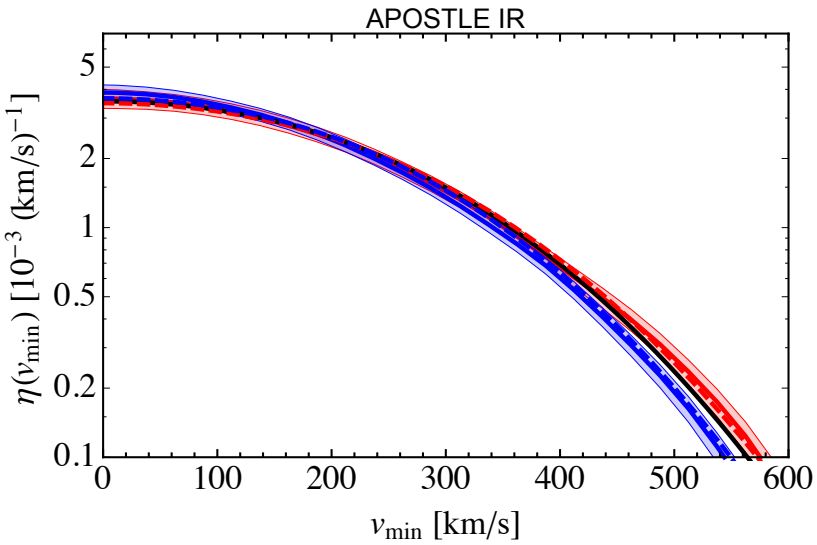

- Significant halo-to-halo scatter in the halo integrals.
- Halo integrals for the best fit Maxwellian velocity distribution fall within the 1σ uncertainty band of the halo integrals of the simulated haloes.
- A Maxwellian velocity distribution with a peak speed constrained by hydrodynamic simulations could be used by the community in the analysis of direct detection data.

The halo integral

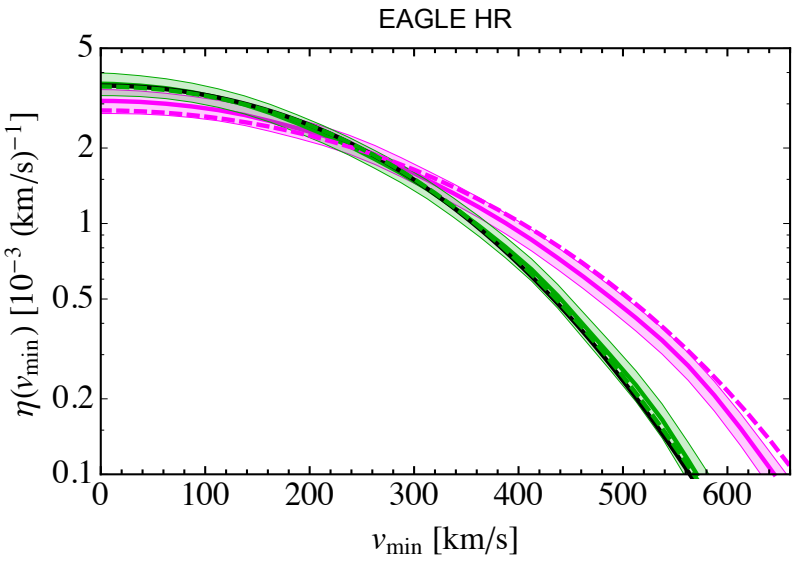

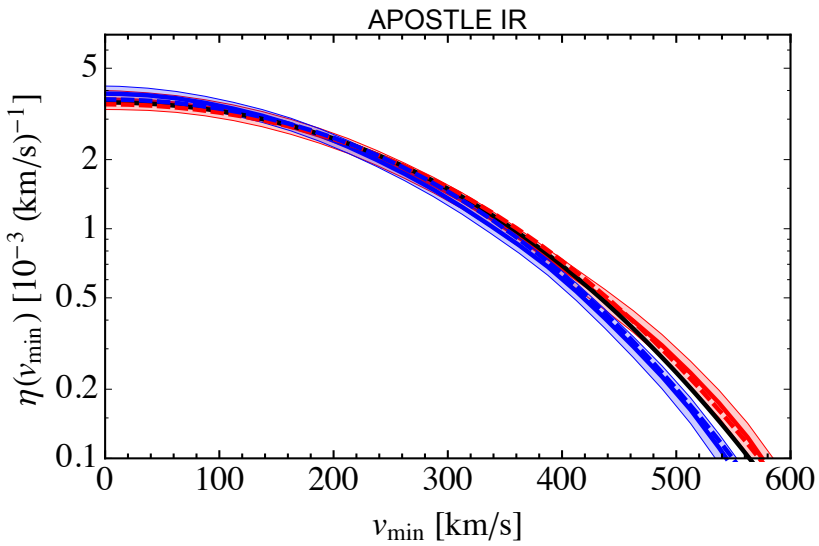

- Comparison to DMO simulations:

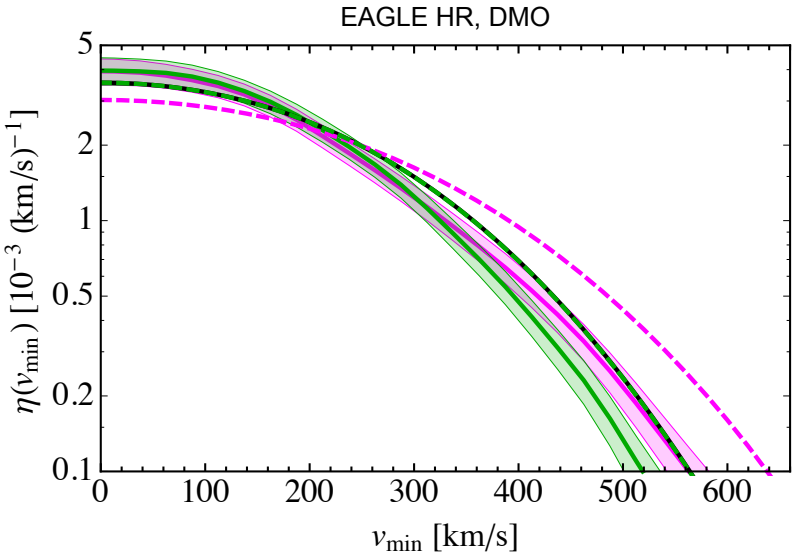

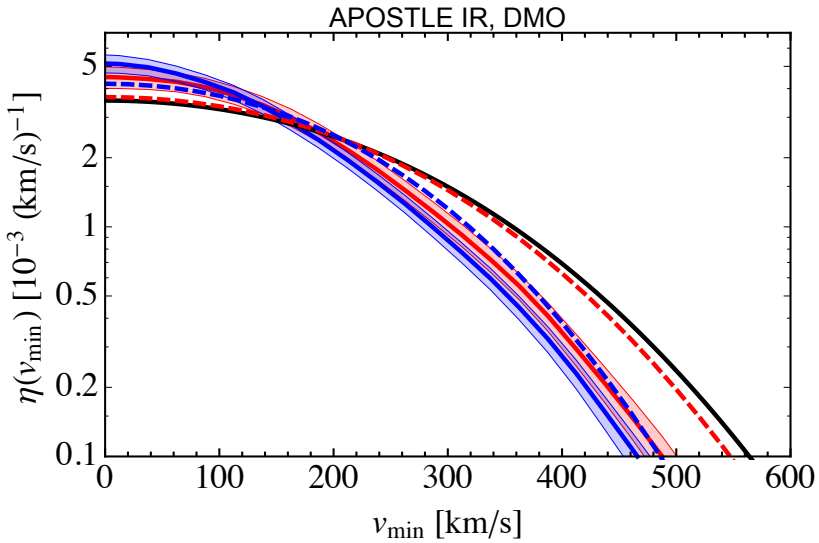

The halo integral

- Including baryons in the simulations results in a shift of the tails of the halo integrals to higher velocities with respect to the DMO case.
- Speed distributions of DMO haloes not captured well by a Maxwellian. Large deficits at the peak, and an excess at low and very high velocities compared to the best fit Maxwellian. $\Rightarrow$ Halo integrals of DMO haloes quite different from best fit Maxwellian halo integrals.

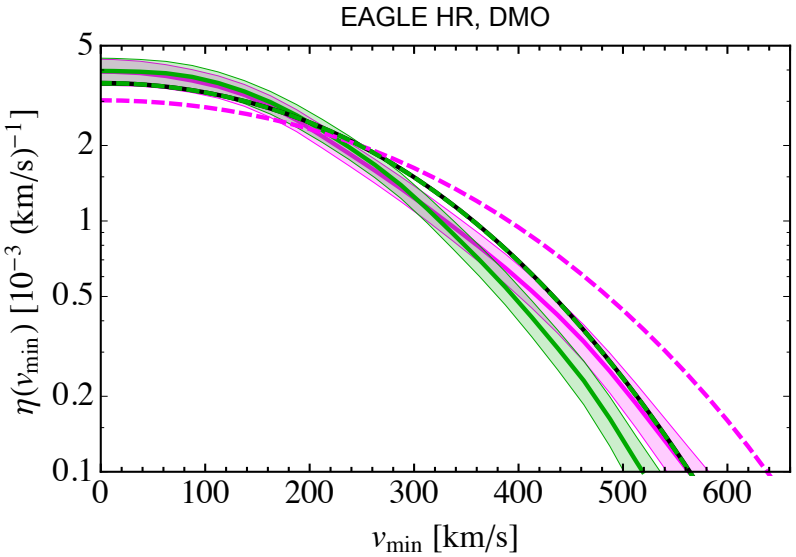

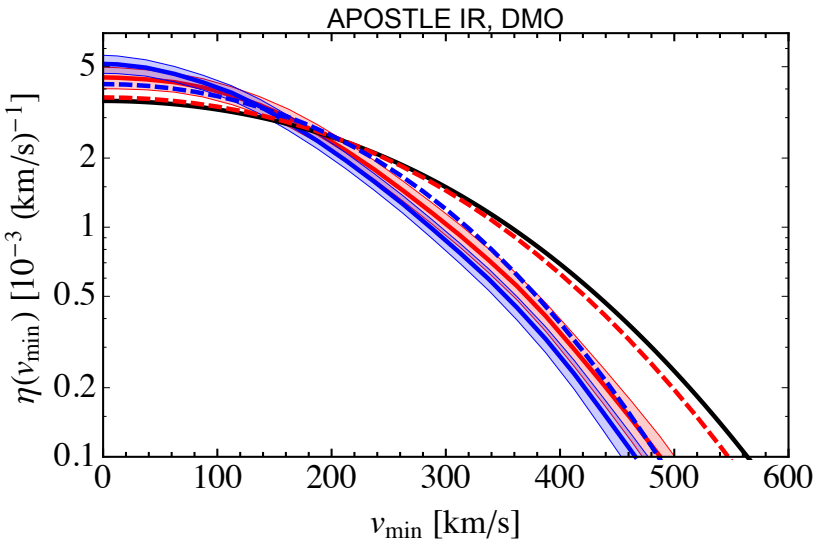

Implications for direct detection

- Assuming the SHM:

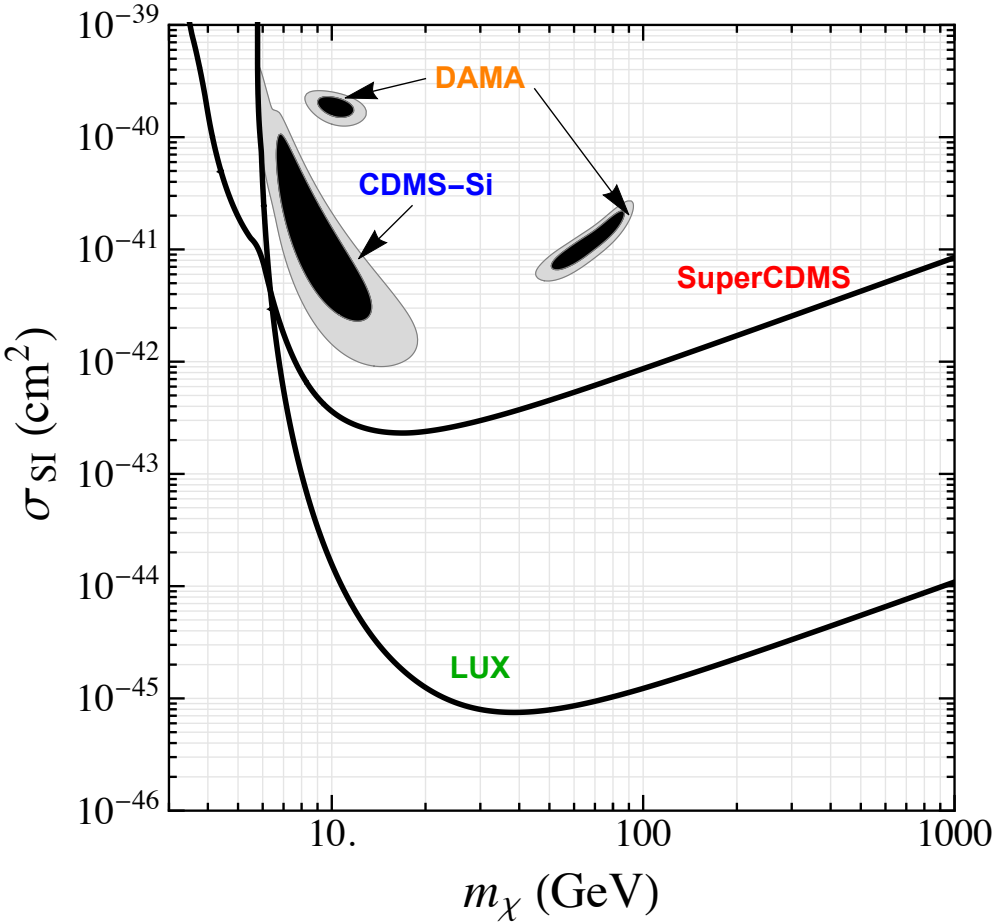

Implications for direct detection

- Comparing with simulated MW-like haloes (smallest ρ_{DM}):

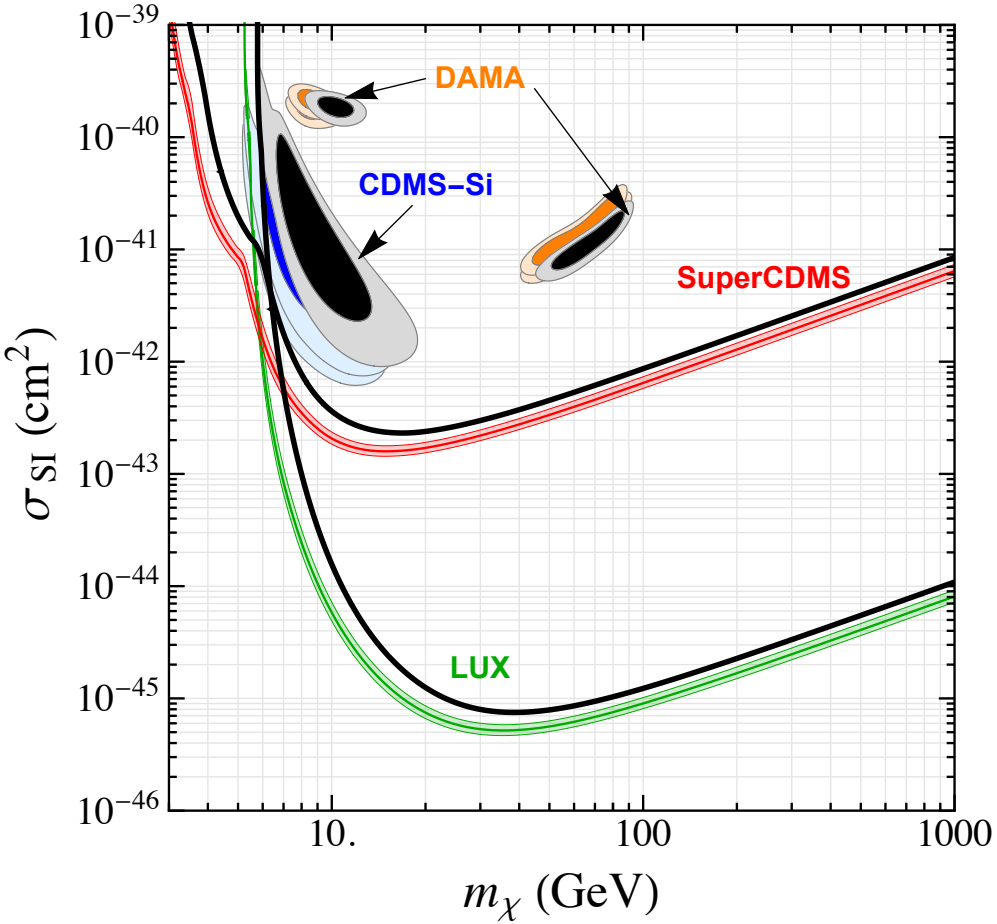

Implications for direct detection

- Comparing with simulated MW-like haloes (largest ρ_{DM}):

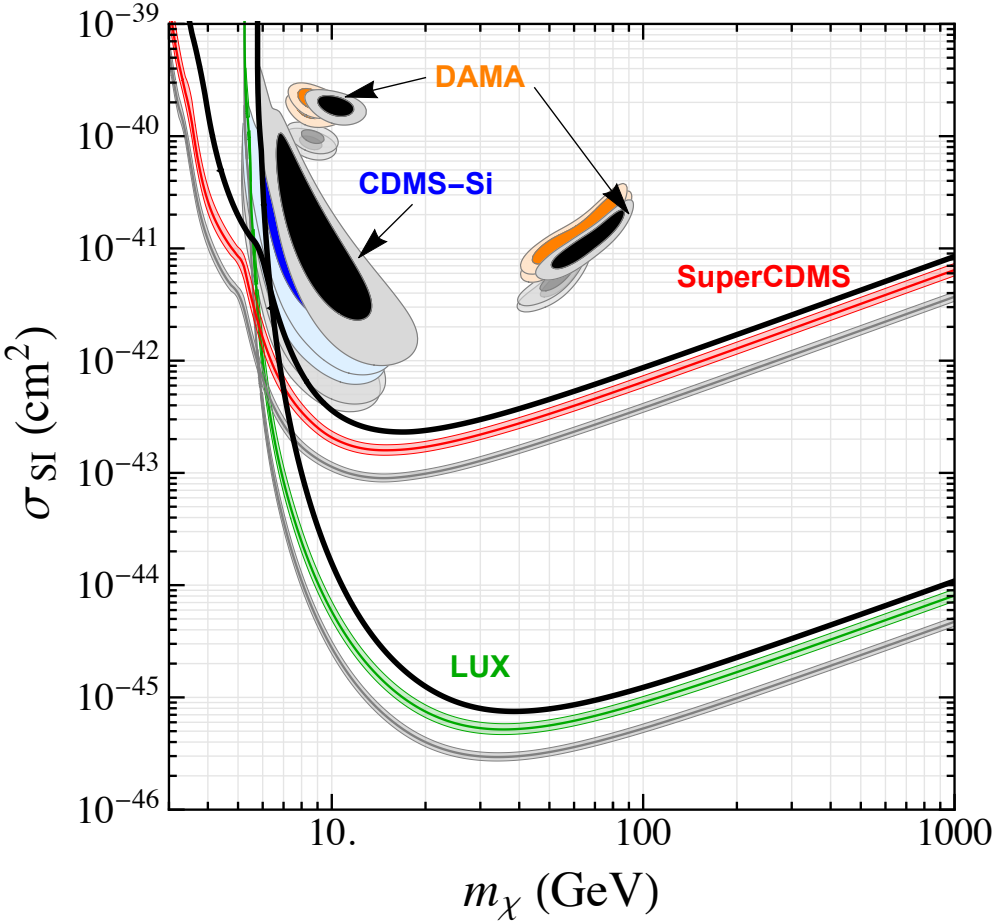

Implications for direct detection

- Comparing with simulated MW-like haloes (largest ρ_{DM}):

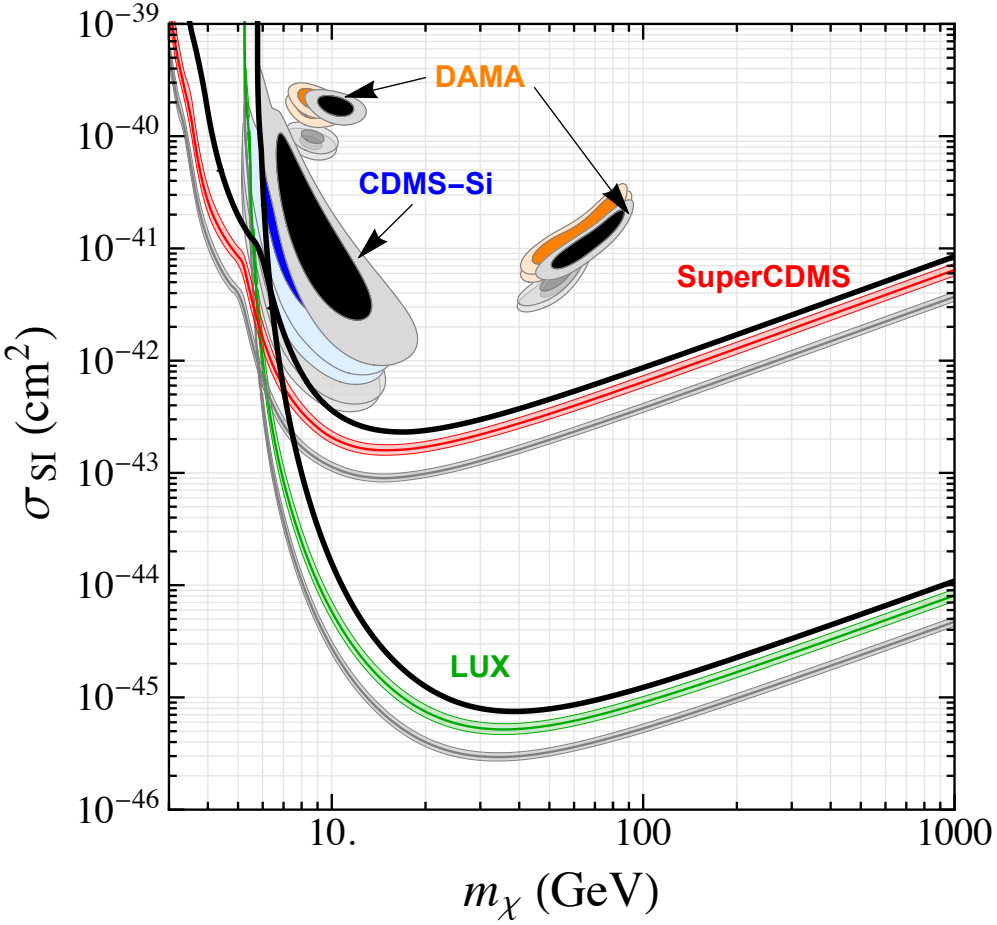

- Halo-to-halo uncertainty larger than the 1σ uncertainty from each halo.

Implications for direct detection

- Comparing with simulated MW-like haloes (largest ρ_{DM}):

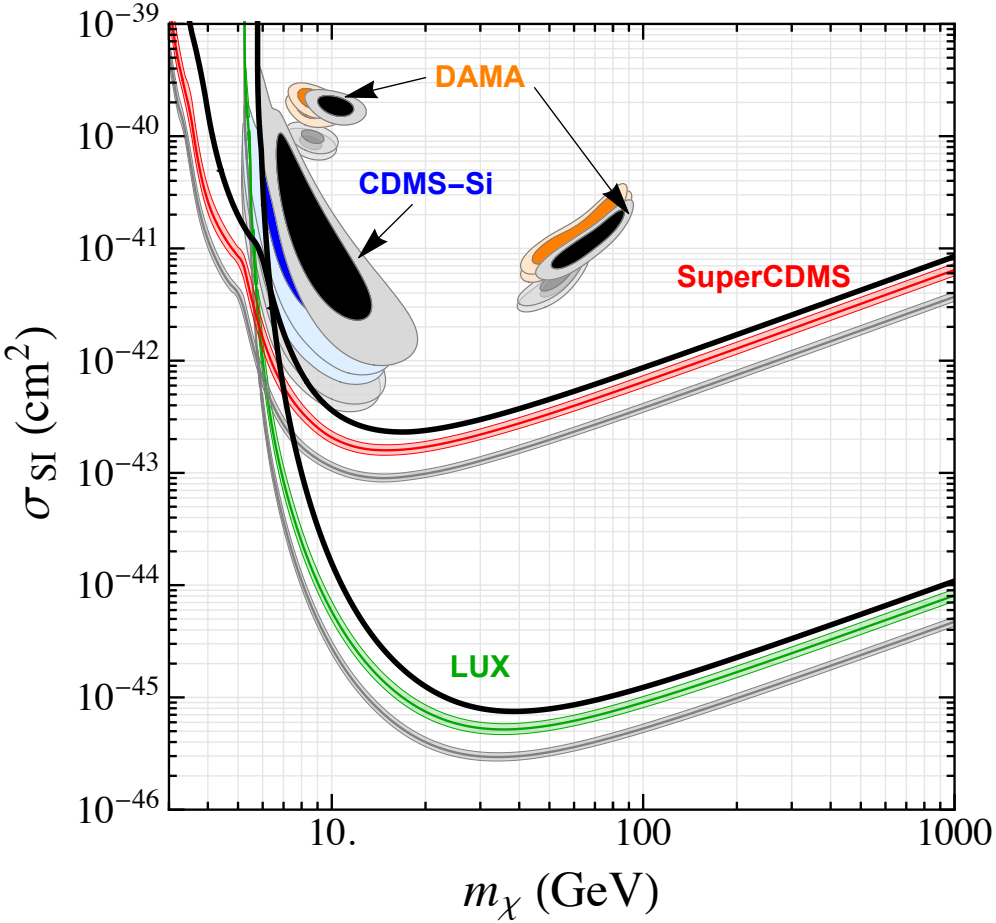

- Halo-to-halo uncertainty larger than the 1σ uncertainty from each halo.
- Overall difference with SHM mainly due to the different local DM density of the simulated haloes.

Effect of the velocity distribution

- Haloes with velocity distributions closest and farthest from SHM Maxwellian:

Fix local $\rho_{\rm DM} = 0.3$ GeV cm^{-3}

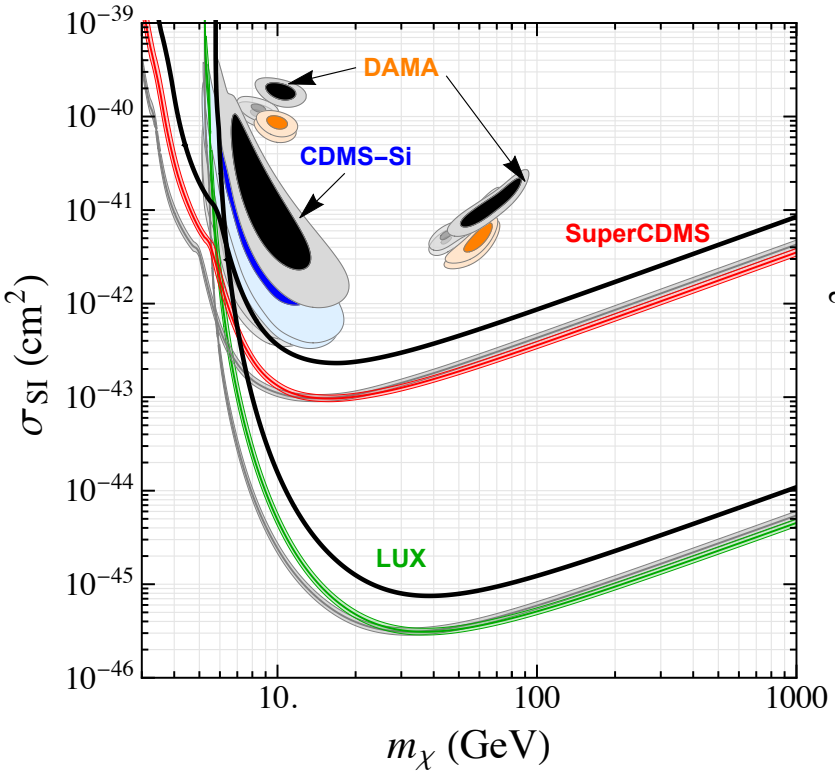

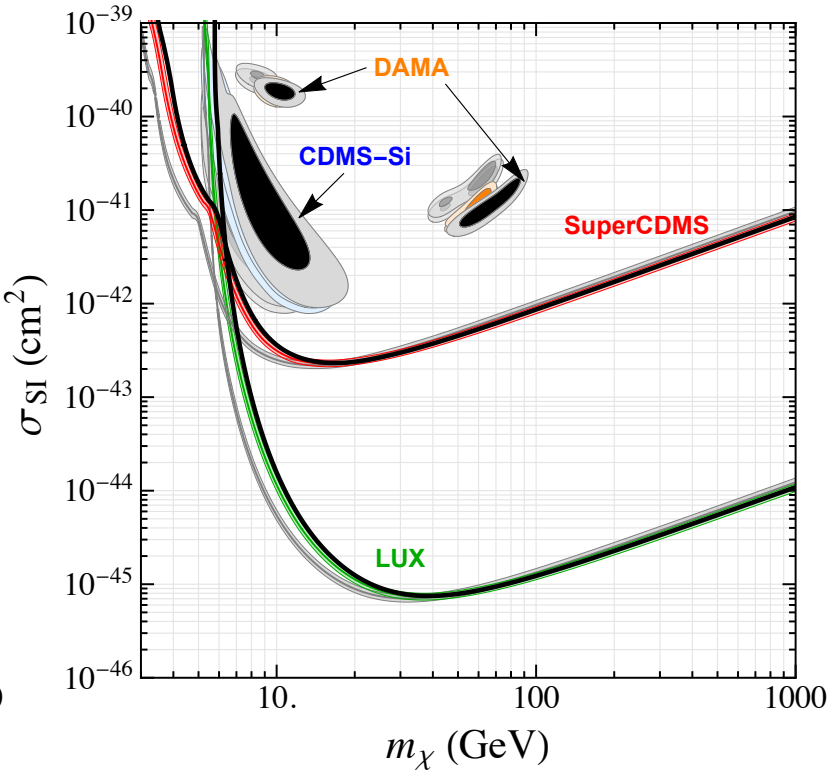

Effect of the velocity distribution

- Haloes with velocity distributions closest and farthest from SHM Maxwellian:

Fix local $\rho_{\rm DM} = 0.3$ GeV cm^{-3}

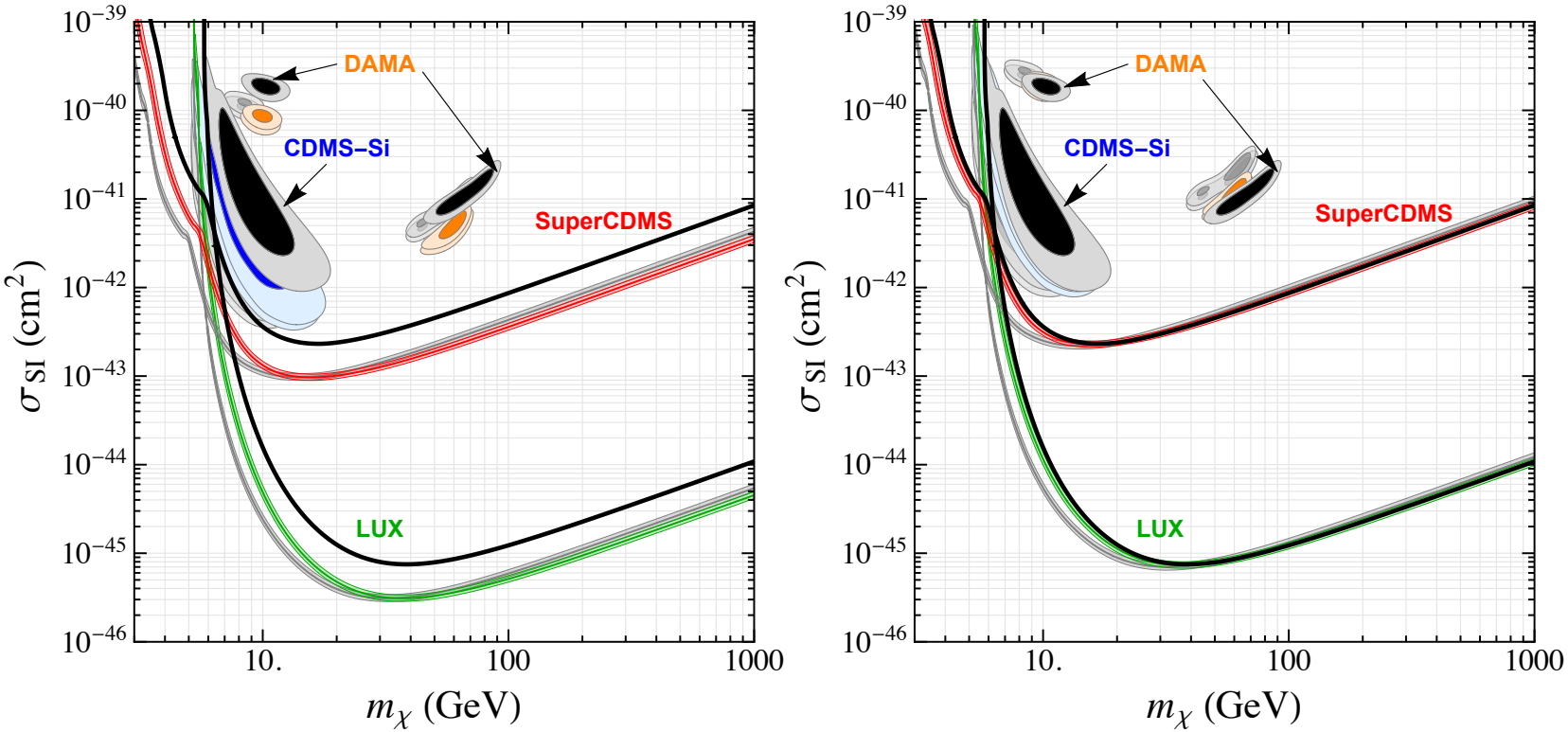

- Shift in the low WIMP mass region persists, where experiments probe the high velocity tail of the distribution.

Comparison with other recent works

- **Kelso et al. 1601.04725** study two MW-like galaxies from the MaGICC simulations. Analogous to our findings, they also find that the best fit Maxwellian velocity distribution provides a good fit to the velocity distribution of each simulated halo.

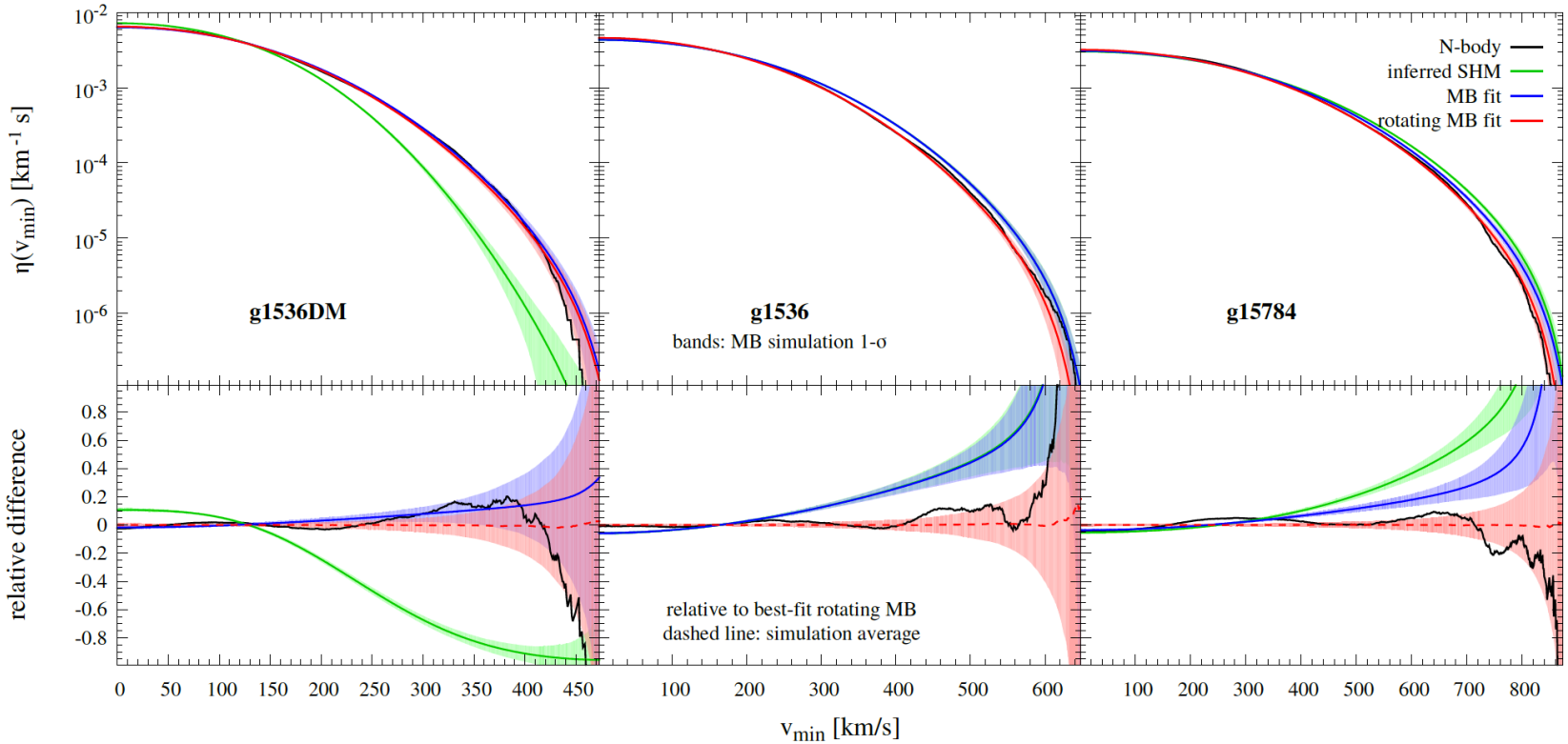

Comparison with other recent works

- **Sloane et al. 1601.05402** study four MW-like galaxies with various merger histories. For most haloes, best fit Maxwellian halo integrals show only small discrepancies at high speeds compared to simulations.

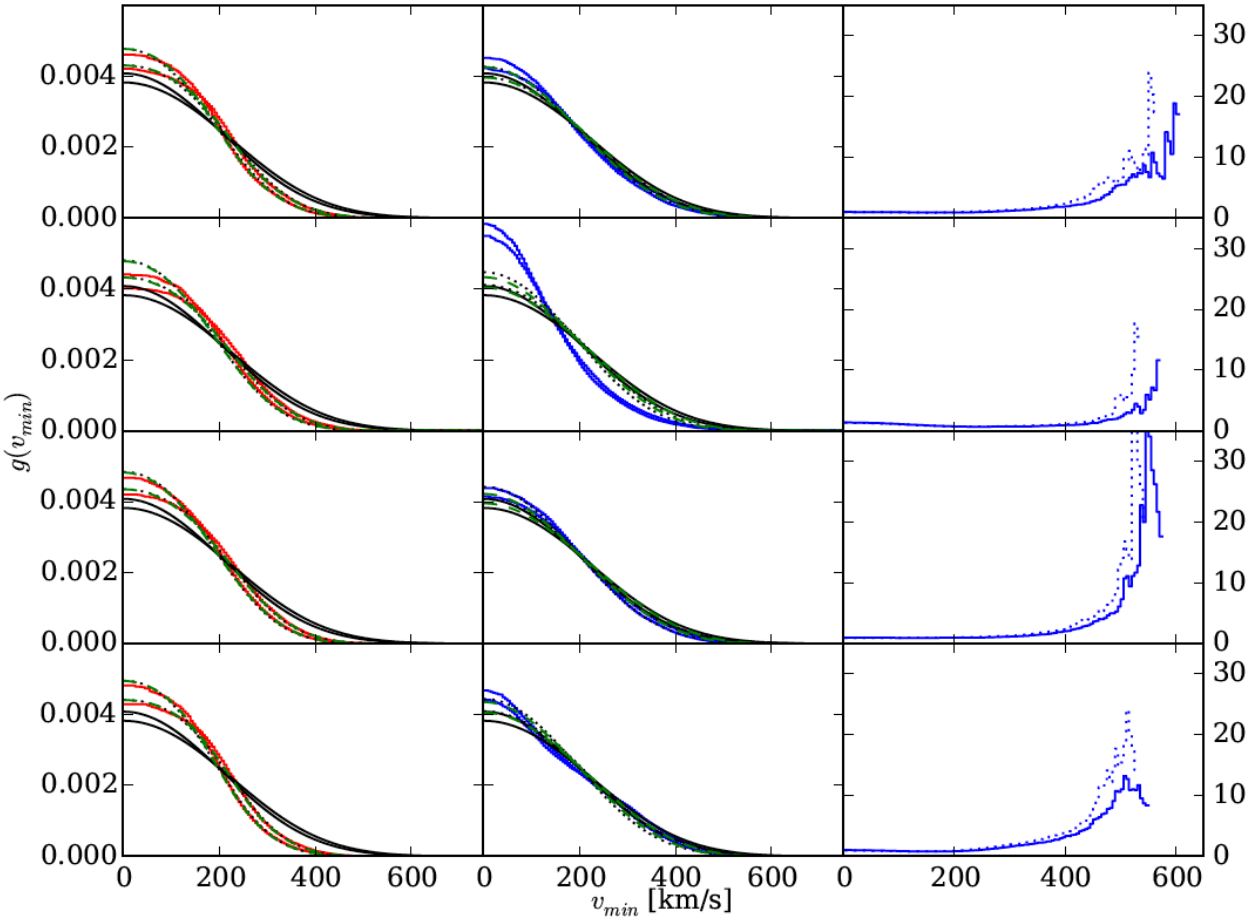

Summary

- We identified simulated haloes which satisfy observational properties of the Milky Way, besides the uncertain mass constraint. Haloes are *MW-like* if:
  - good fit to observed MW rotation curve.
  - stellar mass in the 3σ observed MW stellar mass range.

Summary

- We identified simulated haloes which satisfy observational properties of the Milky Way, besides the uncertain mass constraint. Haloes are *MW-like* if:
  - good fit to observed MW rotation curve.
  - stellar mass in the 3σ observed MW stellar mass range.

- The local DM density: $\rho_{\rm DM} = 0.41 - 0.73$ GeV cm^{-3}. $\Rightarrow$ overall shift of the allowed regions and exclusion limits for all masses.

Summary

- We identified simulated haloes which satisfy observational properties of the Milky Way, besides the uncertain mass constraint. Haloes are *MW-like* if:
  - good fit to observed MW rotation curve.
  - stellar mass in the 3σ observed MW stellar mass range.

- The local DM density: $\rho_{\rm DM} = 0.41 - 0.73$ GeV cm^{-3}. $\Rightarrow$ overall shift of the allowed regions and exclusion limits for all masses.

- Halo integrals of MW analogues match well those obtained from best fit Maxwellian velocity distribution (with mean speed 223 – 289 km/s). $\Rightarrow$ shift of allowed regions and exclusion limits by a few GeV at low DM masses compared to SHM.

Summary

- We identified simulated haloes which satisfy observational properties of the Milky Way, besides the uncertain mass constraint. Haloes are *MW-like* if:
  - good fit to observed MW rotation curve.
  - stellar mass in the 3σ observed MW stellar mass range.

- The local DM density: $\rho_{\rm DM} = 0.41 - 0.73$ GeV cm^{-3}. $\Rightarrow$ overall shift of the allowed regions and exclusion limits for all masses.

- Halo integrals of MW analogues match well those obtained from best fit Maxwellian velocity distribution (with mean speed 223 – 289 km/s). $\Rightarrow$ shift of allowed regions and exclusion limits by a few GeV at low DM masses compared to SHM.

- Shift in the allowed regions and exclusion limits occurs in the same direction. $\Rightarrow$ compatibility between different experiments is not improved.

Additional slides

Selection criteria

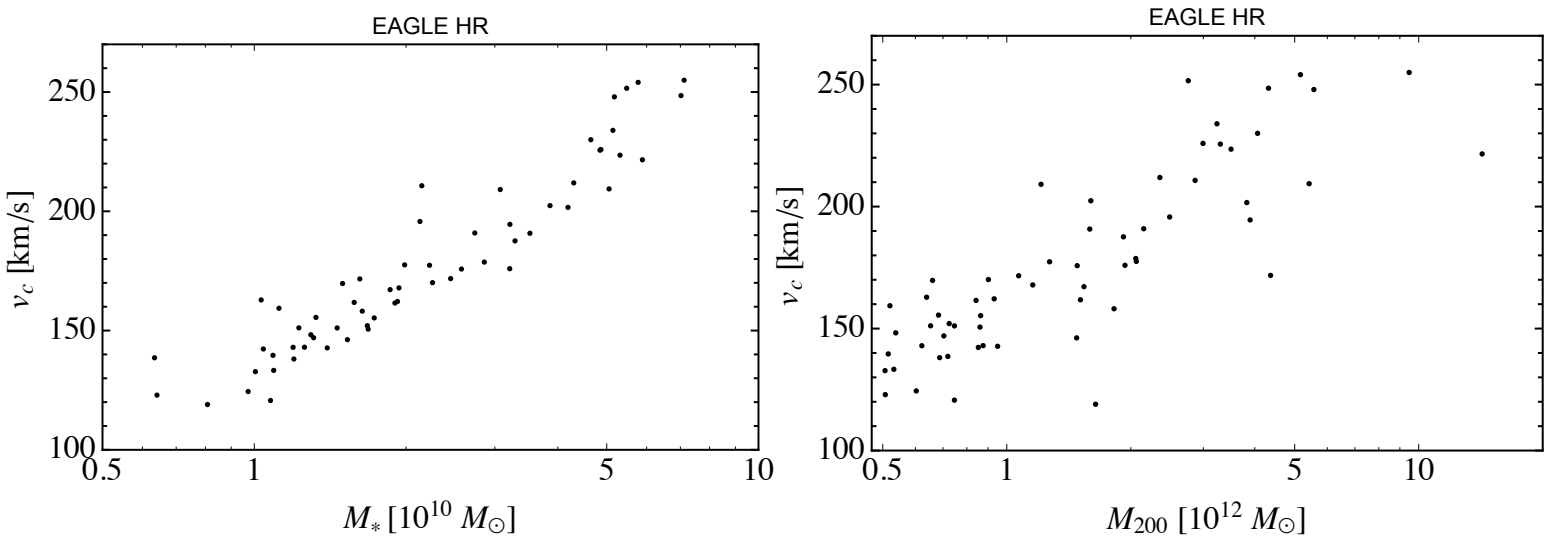

- $M_\star$ strongly correlated with v_c at 8 kpc, while the correlation of M_{200} with v_c is weaker.
- $M_\star(R < 8\ \mathrm{kpc}) = (0.5 - 0.9)M_\star$.
- $M_{\mathrm{tot}}(R < 8\ \mathrm{kpc}) = (0.01 - 0.1)M_{200}$.
- Over the small halo mass range probed, little correlation between $M_{\mathrm{DM}}(R < 8\ \mathrm{kpc})$ and M_{200}.

Velocity distribution azimuthal components

DM and stellar velocity distributions:

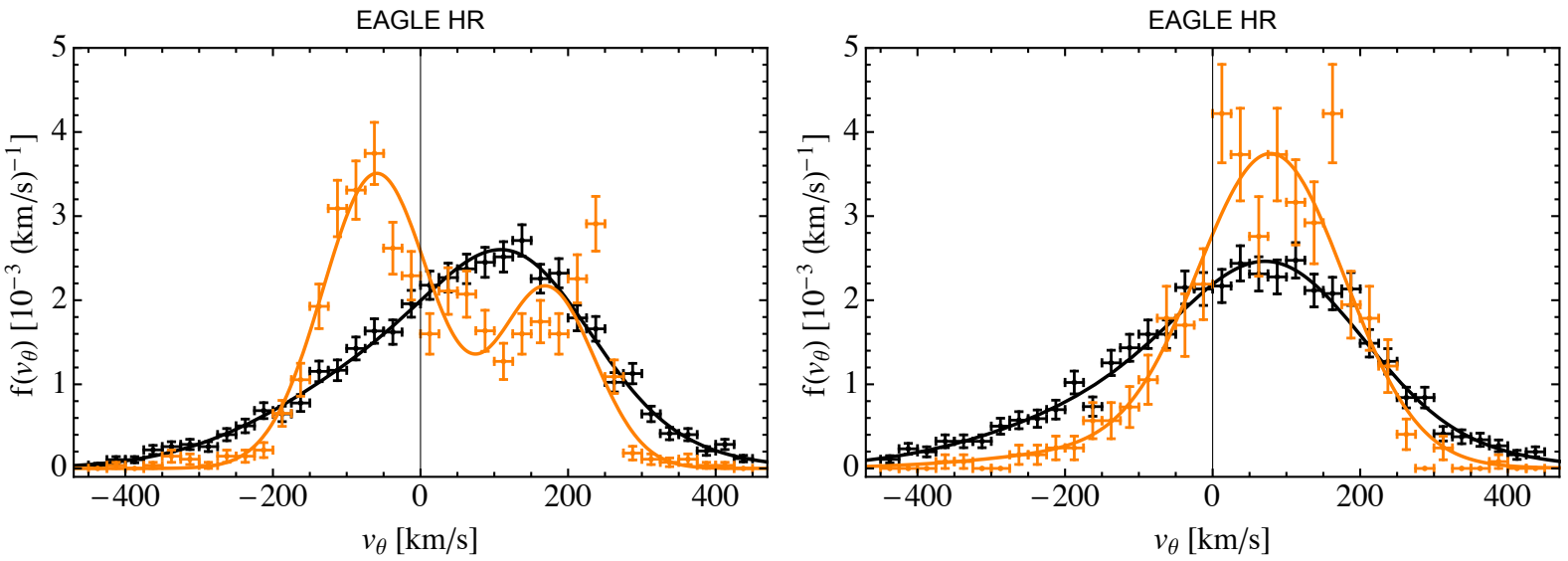

- Fit with a double Gaussian. Difference in the mean speed of second Gaussian between DM and stars is 35 km/s in the left, and 7 km/s in the right panel.
- Fraction of second Gaussian is 32% in the left panel and 43% in the right panel.

Local dark matter density

Is there an enhancement of the local DM density in the **Galactic disc** compared to the **halo**?

- Compare the the average $\rho_{\rm DM}$ in the torus with the value in a spherical shell at $7 < R < 9$ kpc.

  $\rho_{\rm DM}^{\rm torus}$ is larger than $\rho_{\rm DM}^{\rm shell}$ by:

  2 – 27% for 10 haloes,
  greater than 10% for 5 haloes, and
  greater than 20% for only two haloes.

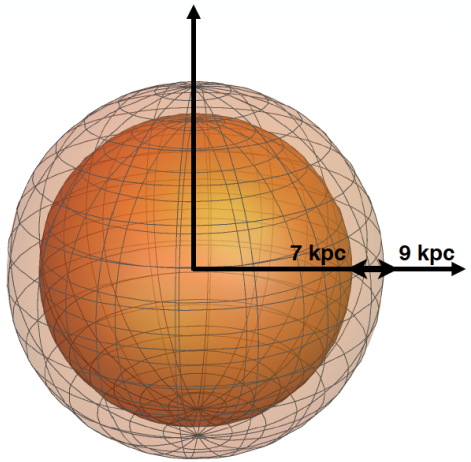

- The increase in the DM density in the disc could be due to the DM halo contraction as a result of dissipational baryonic processes.

Halo shapes

- To study the shape of the inner ($R < 8$ kpc) DM haloes, we calculate the inertia tensor of DM particles within 5 and 8 kpc.
  $\Rightarrow$ ellipsoid with three axes of length $a \geq b \geq c$.

- Calculate the sphericity: $s = c/a$.
  - $s = 1$: perfect sphere. $s < 1$: increasing deviation from sphericity.
  - At 5 kpc, $s = [0.85, 0.95]$. At 8 kpc, s lower by less than 10%.
  - Due to dissipational baryonic processes, DM sphericity systematically higher in the hydrodynamic simulations compared to DMO haloes in which $s = [0.75, 0.85]$.

Halo shapes

- Describe a deviation from sphericity by the triaxiality parameter:

$$T = \frac{a^2 - b^2}{a^2 - c^2}$$

- Oblate systems, $a \approx b \gg c \Rightarrow T \approx 0$.

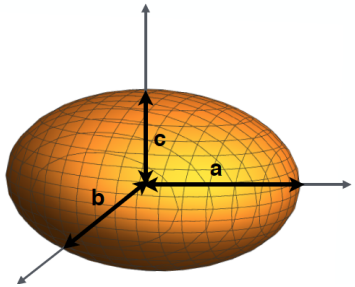

- Prolate systems, $a \gg b \approx c \Rightarrow T \approx 1$.

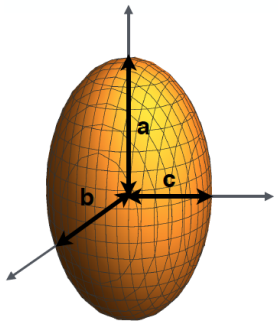

- In the hydro case, since inner haloes are very close to spherical, deviation towards either oblate or prolate is small. DMO counterparts have a preference for *prolate* inner haloes.